

Article

Spatiotemporal Analysis of the Frost Regime in the Iberian Peninsula in the Context of Climate Change (1975–2018)

Abelardo García-Martín ^{1,*} , Luis L. Paniagua ¹ , Francisco J. Moral ² , Francisco J. Rebollo ³ and María A. Rozas ¹ 

- ¹ Departamento de Ingeniería del Medio Agronómico y Forestal, Escuela de Ingenierías Agrarias, Universidad de Extremadura, 06007 Badajoz, Spain; llpsimon@unex.es (L.L.P.); marozas@unex.es (M.A.R.)
- ² Departamento de Expresión Gráfica, Escuela de Ingenierías Industriales, Universidad de Extremadura, 06006 Badajoz, Spain; fjmoral@unex.es
- ³ Departamento de Expresión Gráfica, Escuela de Ingenierías Agrarias, Universidad de Extremadura, 06007 Badajoz, Spain; frebollo@unex.es
- * Correspondence: abgarcia@unex.es; Tel.: +34-9-2428-9600

Abstract: Climate change is having many effects in the agricultural sector, which are being studied worldwide. Undoubtedly, warmer winters and earlier springs produce changes in frost regimes and severity that will affect the sustainability of agricultural production in the area. The Mediterranean region and the Iberian Peninsula (IP) are among the areas where the greatest impact of climate change is expected. Daily data from 68 weather stations of the IP belonging to the European Climate Assessment and Dataset (1975–2018) were used to conduct a spatiotemporal study of the frost regime. The variables calculated include the probability of three frost types according to their severity, frost day, mean absolute minimum yearly temperature, first frost day, last frost day, and frost-free period. These variables were integrated into a geographic information system, which allowed the graphical visualization of their patterns using of geostatistical interpolation techniques (kriging). Changes in frost variables were investigated using the Mann–Kendall test and Sen’s slope estimator. A general reduction in the number of frosts per year is observed (values between -0.04 - and -0.8 -day frosts per year), as well as an increase in the mean absolute minimum temperature (values between 0.04 and 0.10 °C per year), with very high significant trends throughout the territory. The reduction in the number of frosts is more pronounced at a higher elevation. Frost dates vary greatly due to the orographic characteristics of the IP. The generalized trend is of a significant delay of the autumn frosts (values between 0.4 and 1.06 days/year), as well as early spring frosts (between -0.429 and -1.29 days/year), and as a consequence a longer frost-free period, all changes were much stronger than those found in other regions of the world. These effects of climate change must be mitigated by modifying species, varieties, and cultivation techniques to guarantee sustainable agriculture.

Keywords: freezing temperatures; agroclimatology; Mediterranean region; climate trends; spatiotemporal patterns



Citation: García-Martín, A.; Paniagua, L.L.; Moral, F.J.; Rebollo, F.J.; Rozas, M.A. Spatiotemporal Analysis of the Frost Regime in the Iberian Peninsula in the Context of Climate Change (1975–2018). *Sustainability* **2021**, *13*, 8491. <https://doi.org/10.3390/su13158491>

Academic Editor:
Mohammad Valipour

Received: 27 June 2021
Accepted: 26 July 2021
Published: 29 July 2021

Publisher’s Note: MDPI stays neutral with regard to jurisdictional claims in published maps and institutional affiliations.



Copyright: © 2021 by the authors. Licensee MDPI, Basel, Switzerland. This article is an open access article distributed under the terms and conditions of the Creative Commons Attribution (CC BY) license (<https://creativecommons.org/licenses/by/4.0/>).

1. Introduction

Temperatures have a great influence on plants in many ways. Among other climatic variables, critical temperatures and the minimum temperatures that plants can withstand are highly important since they establish the limits of their geographical distribution [1] and considerably influence their development and productive potential [2,3].

The ability of plants to withstand the cold varies from one species to another. While most tropical plants die when exposed to temperatures between 0 and 5 °C, arctic species can withstand temperatures down to -40 °C [4]. Temperate-climate plants occupy an intermediate status. The cold resistance of a particular species is variable depending on the phenological moment in which it is found, with periods of high resistance, for example, of temperate fruit trees during winter dormancy and periods of high sensitivity during the

flowering phase and fruit setting. In this sense, while low winter temperatures can limit the distribution area of crops, low temperatures during spring (Northern Hemisphere) can seriously affect the production of an established crop [5].

Low temperatures and, in particular, frost cause various levels of damage to crops depending on various factors, such as species, cultivar, phenological status, and the duration and intensity of the frost. Numerous studies have analyzed frost damage, indicating that the cold, and in particular frost, are important environmental factors limiting plant productivity and distribution [6–8]. In freeze-risk areas, cold and frost cause significant economic damage [5,9,10]. Snyder and Melo-Andreu (2005) [11] indicated that in Europe, economic losses due to frost are greater than those due to any other climate phenomenon. Specifically, spring frosts cause more economic loss in perennial crops in temperate climates than other unsuitable temperatures [11,12]. In some cases, the damage can be so dramatic that plant production is nearly lost with a single frost event during a sensitive period in its cycle.

Many authors have reported dramatic frost events on different continents, for example, Augspurger [13], Gu et al. [14], and Hufkens et al. [15] in the United States and Ningre and Colin [16] and Kreyling et al. [17] in Europe. In most cases, these events occurred after an abnormally warm period that sped up the phenological cycle of plants in spring [18]. Autumn frosts can also cause significant damage, especially in plants that have not yet entered dormancy [1].

According to the Group of Insurance Companies for Combined Agrarian Insurance of Spain [19,20], the frost damage declared during 2018 produced losses amounting to 60 million euros in February, March, and early May. In 2019, frost damage was declared again in January, March, and early May, resulting in losses of 48.7 million euros.

Knowledge of frost risk has been useful for making decisions on land use and the management of frost-sensitive crops. Extreme temperatures can have a great impact on crop production and planning. In summer crops, their planting date depends on the last frost date [21,22]. For winter crops, delays in the last frost of the season can greatly affect yields [22], so frosts also impact the sowing dates of these crops.

The warming produced by global climate change raises the uncertainty about the future climate, with several possible scenarios being proposed, since the variables to consider (including human activities) are many and exist in a very complicated global context. The fate of some areas of the world, because of certain characteristics such as their geographical position or orographic diversity, as occurs with the Iberian Peninsula (IP) and the Mediterranean basin in general, presents a great degree of uncertainty [23–25].

Since the mid-1980s, there has been a debate about whether the frequency of frost, its severity, and thus the risk of frost damage in temperate climates will increase or decrease in the coming decades. Higher air temperatures due to climate change generally reduced the total number of frost days per year and lengthened the frost-free season [26–28]. On the other hand, there is no consensus that the occurrence and severity of spring frosts decrease due to global warming [18].

One consequence that can be expected from the climate change-driven temperature increase is the change in plant phenology. Several studies have shown a change in phenological events. For example, Menzel and Fabian [29] found that although the spring events were finishing earlier in Europe, the autumn events were delayed, leading the growing season to be 10.8 days longer. Parmesan and Yohe [30], in a review carried out on a global scale, detected tendencies towards phenological advancement in spring for plant species and for animal species. Badeck et al. [31] found spring phenology events advanced several days per decade in the middle and high latitudes of Europe and found that this advance paralleled the global warming trend. Ge et al. [32] found that although the beginning of spring had advanced since 1996, in the last four years under study, it had been delayed; in contrast, the end of the growing season was later than it had been since 1993. Cleland et al. [33] and Menzel et al. [34] showed that 78% of all flowering and fruiting phenological records were earlier (30% significantly), and only 3% were significantly

delayed, while the end-of-season trigger was ambiguous. Han et al. [35] indicated that earlier budding throughout Europe also depended on latitude and humidity conditions.

Recently, Liu et al. [36] found that the regions experiencing the most dramatic lengthening of the growing season had also had an increased number of frost days during that season, especially in spring, over the last three decades, despite global warming. These two factors bring a very clear increase in frost risk for vegetation.

The growing risk of exposure to frost could be accentuated in the future since maximum temperatures are still increasing faster than minimum temperatures, causing a phenological advancement [37]. This phenological advance implies an increased risk of damage to developing flowers and freshly set fruits, which are also very sensitive to cold temperatures. In agreement with Vitasse et al. [18], the risk of spring frosts increased due to earlier flowering, especially at elevations above 800 m. All of the above results indicate that variations in growing season length, as well as the time at which frosts occur, can be good indicators of climate change, as indicated by Robeson [26] and Easterling et al. [38].

Temperatures measured from a weather station may not be useful for evaluating the risk of frost at the plot level in areas with diverse topography: The risk of frost at any given site could differ significantly from that recorded in the closest station. Particular topographic conditions can cause large temperature differences and therefore different frost-risks [39,40]. Therefore, it is necessary to create models that incorporate spatial information to extend the knowledge of minimum temperatures and the risk of frost [41–44]. In recent decades, geospatial techniques have gained considerable interest among the scientific community in the studying of Earth and hydrological sciences to solve and understand various problems and develop complex approaches in natural resource management [45]. These techniques have been successful for decision-making in agricultural management to minimize risks.

Despite the influence of frost on the distribution and productivity of crops and the importance of the agricultural sector on the IP, no studies have analyzed the frost regime and its trend in the context of climate change due to global warming. The objective of this research is to conduct a spatial and temporal analysis of the frost regime in the IP. We determine the frequency of frosts according to their intensity, minimum temperatures, and the number of frosts and the distribution of frosts according to their intensity, dates of the first and last frosts of the season, duration of the frost as well as frost-free periods. We also identify and quantify the trends of these variables during the years of study.

2. Materials and Methods

2.1. Study Area

The study area of this work is the IP, a geographical area of southwest Europe consisting of Spain and Portugal. The IP is located in a prominent place within the general atmospheric circulation, which does not remain static but rather has different movements from north to south, depending on the season. The Peninsula is in a temperate zone and does not have homogeneous climatic characteristics. It is a mixing zone between zones of warm air and zones of cold air (subtropical and polar). In addition, the varied orography of Spain gives it a marked climatic diversity.

The main feature is a wide central plateau (Meseta Central) with a mean elevation of 660 m divided by a mountain range (Cordillera Central) and surrounded by other mountain ranges. It presents two large depressions of the Guadalquivir and Ebro Rivers. According to the classification of Beck et al. [46], there are four large climatic groups. Most of the center and south have temperate climates with very dry, hot summers. The northwest of the Peninsula, as well as most of the west coast of Portugal and numerous mountainous areas of the interior of the Peninsula, has a temperate climate with dry and temperate summers. In the Cantabrian region, in the Iberian System, part of the northern plateau, and much of the Pyrenees except for the highest parts, the climate is temperate climate without a dry season and mild summers. In the east, southeast, and center, we find areas with cold steppe climates. Elevation determines other microclimates along the IP [47].

2.2. Database and Interpolation Method

From 68 stations contained in the European Climate Assessment & Dataset (ECA&D) [48–50], we took the daily maximum and minimum temperatures and precipitation for the period 1975–2017. The quality control procedures of the Algorithm Theoretical Basis Document project, developed by the Royal Netherlands Meteorological Institute for the ECA&D, have been applied to this ECA&D database [48]. The blended series passed the standard homogeneity test, the Buishand range test, the Pettitt test, and the Von Neumann ratio test, as described by Wijngaard et al. [51] and ECA&D [48]. Some series presenting missing values were completed following the recommendations of the WMO [52] and Allen et al. [53].

The daily data from each station were processed and analyzed, and the annual values for each of the indices used in this study were calculated. The locations of all stations selected are shown in Figure 1, and their detailed geographical locations are shown in Table 1.

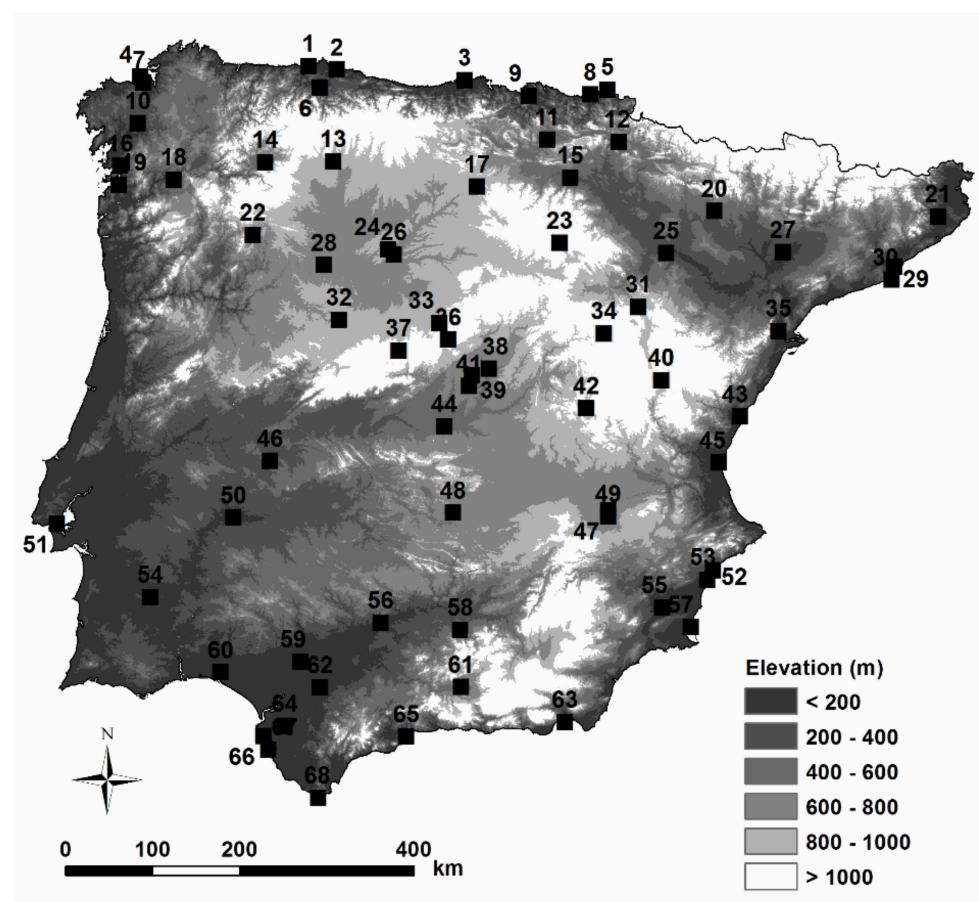


Figure 1. Digital elevation model of the Iberian Peninsula and location of weather stations used in this study.

Table 1. Elevation and geographic coordinates of the selected weather stations from the Iberian Peninsula. The numbers in Figure 1 correspond to the station numbers in the table.

No	Station	Elevation (m)	Latitude (°N)	Longitude (+°E, −°W)	No	Station	Elevation (m)	Latitude (°N)	Longitude (+°E, −°W)
1	Avilés	127	43.57	−6.04	35	Tortosa	44	40.82	0.49
2	Gijón	3	43.54	−5.64	36	Navacerrada	1894	40.78	−4.01
3	Santander	64	43.46	−3.82	37	Ávila	1130	40.66	−4.68
4	Coruña	58	43.37	−8.42	38	Torrejón	611	40.48	−3.45
5	Fuenterrabía	4	43.36	−1.79	39	Madrid	667	40.41	−3.68

Table 1. Cont.

No	Station	Elevation Latitude Longitude			No	Station	Elevation Latitude Longitude		
		(m)	(°N)	(+°E, −°W)			(m)	(°N)	(+°E, −°W)
6	Oviedo	336	43.35	−5.87	40	Teruel	900	40.35	−1.12
7	Alvedro	98	43.31	−8.37	41	Getafe	617	40.30	−3.72
8	Igueldo	251	43.31	−2.04	42	Cuenca	945	40.07	−2.14
9	Bilbao	42	43.30	−2.91	43	Castellón	35	39.95	−0.07
10	Santiago de Compostela	370	42.89	−8.41	44	Toledo	515	39.88	−4.05
11	Vitoria	521	42.85	−2.65	45	Cáceres	459	39.48	−6.37
12	Pamplona	442	42.82	−1.64	46	Valencia	11	39.48	−0.37
13	León	916	42.59	−5.65	47	Albacete	674	39.01	−1.86
14	Ponferrada	534	42.56	−6.6	48	Ciudad Real	628	38.99	−3.92
15	Agoncillo	353	42.45	−2.33	49	Los Llanos	704	38.95	−1.86
16	Pontevedra	108	42.44	−8.62	50	Talavera la Real	185	38.88	−6.83
17	Villafraía	890	42.36	−3.63	51	Lisboa	77	38.72	−9.15
18	Ourense	143	42.33	−7.86	52	Alicante	81	38.37	−0.49
19	Vigo	261	42.24	−8.62	53	Alicante	43	38.28	−0.57
20	Huesca	541	42.08	−0.33	54	Beja	246	38.02	−7.87
21	Girona	143	41.91	2.76	55	Murcia	61	38.00	−1.17
22	Braganza	690	41.80	−6.73	56	Córdoba	90	37.84	−4.85
23	Soria	1082	41.78	−2.48	57	San Javier	4	37.79	−0.8
24	Villanubla	846	41.70	−4.85	58	Jaén	582	37.78	−3.81
25	Zaragoza	247	41.66	−1.01	59	Sevilla	34	37.42	−5.88
26	Valladolid	735	41.65	−4.77	60	Huelva	19	37.28	−6.91
27	Lleida	192	41.63	0.60	61	Granada	567	37.19	−3.79
28	Zamora	656	41.52	−5.73	62	Morón de la Frontera	87	37.16	−5.62
29	Barcelona	412	41.42	2.12	63	Almería	7	36.83	−2.45
30	Barcelona	4	41.29	2.07	64	Jerez de la Frontera	27	36.75	−6.06
31	Daroca	779	41.11	−1.41	65	Málaga	7	36.67	−4.49
32	Salamanca	790	40.96	−5.50	66	Rota	21	36.64	−6.33
33	Segovia	1005	40.95	−4.13	67	Cádiz	1	36.50	−6.26
34	Molina de Aragón	1056	40.84	−1.89	68	Tarifa	32	36.02	−5.6

With the aim of estimating at any location, a geostatistical algorithm was selected. Concretely, the regression kriging algorithm was used. It is indicated to use this when the auxiliary data are available everywhere across the study area [54].

Predictions using regression kriging are made separately for the trend and residuals and then added back together. In consequence, any variable at a new unsampled point, x , is $Z_{RK}^*(x)$ estimated, using regression kriging as follows:

$$Z_{RK}^*(x) = m(x) + r(x) \quad (1)$$

where the trend, $m(x)$, is fitted using linear regression analysis and the residuals, $r(x)$, are estimated using an ordinary kriging algorithm. Thus, the prediction is made by:

$$Z_{RK}^*(x) = \sum_{j=0}^p c_j \cdot v_j(x) + \sum_{i=1}^n w_i(x) \cdot r(x_i) \quad (2)$$

$$v_0(x) = 1 \quad (3)$$

where c_j is the coefficients of the estimated trend model, $v_j(x)$ is the j th predictor at location x , p is the number of predictors, and $w_i(x)$ is the weights determined by solving the ordinary kriging system of the regression residuals, $r(x_i)$, for the n sample points.

In this case study, only one predictor is used, elevation (h), so $m(x) = a + b h(x)$. Latitude was not incorporated into the model, because only in one variable (frost probability) was a significant correlation obtained, and it did not achieve appreciable improvement in the model. In consequence,

$$Z_{RK}^*(x) = a + b \cdot h(x) + \sum_{i=1}^n w_i(x) \cdot r(x_i) \quad (4)$$

The residual at each sampling point, $r(x_i)$, is calculated as the difference between the value of the considered variable and the estimate by the trend ($r(x_i) = Z(x_i) - m(x_i)$).

The elevation was extracted from a digital elevation model (DEM) for the Iberian Peninsula, in the raster format at a 1000×1000 m resolution. Thus, from point data at sampling locations, that is, meteorological stations, estimates can be obtained at any other unsampled location. Once the model is integrated, it is used to produce a continuous surface that allows the determination of values for each variable in each of the pixels. Digital models for each variable, in the raster format at a resolution of 1000×1000 m, were generated. All operations, including the spatial representation and visualization of the variables, were conducted in the GIS software ArcGIS v. 10.3. The geostatistical analysis was performed with the extension Geostatistical Analyst of ArcGIS.

2.3. Frost Indices

The following indices widely used in the scientific literature were determined.

2.3.1. Annual Frost Probability (%)

Annual frost probability indicates the annual probability of frost occurrence when the minimum daily temperature (TN) falls below 0°C . In addition, three categories of frost severity were defined according to Hornstein [55], Ouellet [56], and WMO [57]: Light frosts ($-1.1^\circ\text{C} < \text{TN} < 0^\circ\text{C}$), moderate frosts ($-1.1^\circ\text{C} < \text{TN} < -2.2^\circ\text{C}$), and severe frosts ($\text{TN} < -2.2^\circ\text{C}$).

2.3.2. Frost Days (FD)

FD indicates the number of days per year in which $\text{TN} < 0^\circ\text{C}$. The mean number of light frosts ($-1.1^\circ\text{C} < \text{TN} < 0^\circ\text{C}$), moderate frosts ($-1.1^\circ\text{C} < \text{TN} < -2.2^\circ\text{C}$), and severe frosts ($\text{TN} < -2.2^\circ\text{C}$) per year were calculated. In the years in which there were no frosts in some weather station, the value of frost days was zero, and that year it was not taken into account for the frost dates.

2.3.3. Mean Minimum Yearly Temperature (TMN)

TMN is defined as the mean of the annual minimums in the period considered (1977–2018) and expresses the severity of the winter period.

2.3.4. First Frost Day (FFD)

FFD is the date of the first $\text{TN} < 0^\circ\text{C}$ on or after October 1 and is measured in the form of Julian days. These frosts are generally called autumnal and determine the beginning of the cold period. This starting date was set because no frost was found before it.

2.3.5. Last Frost Day (LFD)

LFD is the date of the last $\text{TN} < 0^\circ\text{C}$ on or after 1 January, counted in Julian days. These frosts are generally called spring frosts and determine the end of the cold period and the beginning of the growing period, causing serious damage to crops when they are very late.

2.3.6. Frost-Free Period (FFP)

FFP is defined as the number of days between LFD and FFD each year. It determines the length of the growth period of the crops.

2.4. Trend Tests: Mann–Kendall Test (MK) and Sen's Estimator

To evaluate the monotonic tendencies of each frost index over time, the Mann–Kendall non-parametric test was used [58,59], as recommended by the WMO [60].

Sen's non-parametric method [61] was used to identify the gradients and their directions. MAKESENS 1.0 is a computer model introduced by Salmi et al. [62], and it was built using Microsoft Excel 97 and macros coded with the Microsoft Visual Basic language.

3. Results and Discussion

3.1. Probability of Frost

The probability of frost, expressed as the percentage of years with frost (Table 2), showed great differences between the weather stations sampled in agreement with Moletisi et al. [63]. Although, the vast majority of them had high or very high values. At 41 of the 68 stations, the probability was 90%; at 55, the probability of frost was greater than 50%; and at only five stations, along the coast, the mean probability of frost was 20% or lower (Figure 2).

The incidence of frost on the IP was high at the vast majority of the stations. This probability was significantly correlated ($p < 0.01$) with the elevation ($r = 0.575$) and latitude ($r = 0.439$) of the weather station. In Figure 2, we can see that the areas of the Mediterranean and Atlantic coasts had a low probability of frost, but this probability was higher on the north coast than on the south due to the effect of latitude.

On the other hand, the vast majority of the interior peninsular surface had a high probability of frost. This will limit the presence of frost-sensitive crops at some point in their growth cycles, reducing their possibility of cultivation to areas near the coast and at low elevations, especially in the Gulf of Cádiz (southwest coast) and the Mediterranean coast in Valencia and Murcia (southeast). These results are consistent with those found by Núñez et al. [64] for 2002–2012.

Table 2. Frost probability (FP), light frost probability (LF), moderate frost probability (MF), and severe frost probability (SF) per selected station in the Iberian Peninsula (1975–2018).

No	Station	FP	LP	MF	SF	No	Station	FP	LP	MF	SF
		%	%	%	%			%	%	%	%
1	Avilés	75.6	73.2	36.6	12.2	35	Tortosa	82.9	78.0	39.0	14.6
2	Gijón	68.3	68.3	41.5	22.0	36	Navacerrada	100.0	100.0	100.0	100.0
3	Santander	19.5	19.5	2.4	0.0	37	Ávila	100.0	100.0	100.0	100.0
4	Coruña	4.9	4.9	0.0	0.0	38	Torrejón	100.0	100.0	100.0	100.0
5	Fuenterrabía	97.6	97.6	87.8	75.6	39	Madrid	97.6	97.6	87.8	61.0
6	Oviedo	92.7	87.8	70.7	51.2	40	Teruel	100.0	100.0	100.0	100.0
7	Alvedro	97.6	97.6	80.5	56.1	41	Getafe	100.0	100.0	97.6	95.1
8	Igueldo	90.2	82.9	68.3	53.7	42	Cuenca	100.0	100.0	100.0	100.0
9	Bilbao	97.6	97.6	75.6	68.3	43	Castellón	39.0	39.0	17.1	4.9
10	Santiago	100.0	100.0	95.1	75.6	44	Toledo	100.0	97.6	100.0	100.0
11	Vitoria	100.0	100.0	100.0	100.0	45	Cáceres	90.2	90.2	70.7	61.0
12	Pamplona	100.0	100.0	100.0	100.0	46	Valencia	22.0	19.5	7.3	2.4
13	León	100.0	100.0	100.0	100.0	47	Albacete	100.0	100.0	100.0	97.6
14	Ponferrada	100.0	100.0	97.6	100.0	48	Ciudad Real	100.0	100.0	100.0	95.1
15	Agoncillo	100.0	100.0	100.0	95.1	49	Los Llanos	100.0	100.0	100.0	100.0
16	Pontevedra	65.9	61.0	39.0	9.8	50	Talavera la Real	97.6	95.1	92.7	82.9
17	Villafria	100.0	100.0	100.0	100.0	51	Lisboa	2.4	0.0	0.0	2.4
18	Ourense	97.6	97.6	90.2	90.2	52	Alicante	36.6	34.1	17.1	2.4
19	Vigo	80.5	78.0	31.7	12.2	53	Alicante	43.9	36.6	22.0	4.9
20	Huesca	100.0	100.0	97.6	97.6	54	Beja	57.1	52.4	31.0	19.0
21	Girona	100.0	100.0	100.0	100.0	55	Murcia	82.9	78.0	63.4	39.0
22	Braganza	100.0	100.0	100.0	100.0	56	Córdoba	92.5	90.0	65.0	57.5
23	Soria	100.0	100.0	100.0	100.0	57	San Javier	78.0	65.9	29.3	14.6
24	Villanubla	100.0	100.0	100.0	100.0	58	Jaén	85.0	80.0	55.0	47.5
25	Zaragoza	100.0	100.0	95.1	90.2	59	Sevilla	56.1	56.1	29.3	19.5
26	Valladolid	100.0	100.0	100.0	100.0	60	Huelva	46.3	46.3	12.2	4.9
27	Lleida	100.0	100.0	100.0	100.0	61	Granada	100.0	100.0	97.6	97.6
28	Zamora	100.0	100.0	100.0	97.6	62	Morón de la Frontera	85.4	80.5	65.9	51.2
29	Barcelona	78.0	78.0	41.5	34.1	63	Almería	2.4	0.0	0.0	2.4
30	Barcelona	78.0	73.2	56.1	19.5	64	Jerez de la Frontera	73.2	68.3	36.6	31.7
31	Daroca	100.0	100.0	100.0	100.0	65	Málaga	19.5	14.6	7.3	2.4
32	Salamanca	100.0	100.0	100.0	100.0	66	Rota	43.9	39.0	22.0	9.8
33	Segovia	100.0	100.0	100.0	97.6	67	Cádiz	4.9	2.4	4.9	2.4
34	Molina de Aragón	100.0	100.0	100.0	100.0	68	Tarifa	2.4	0.0	0.0	2.4

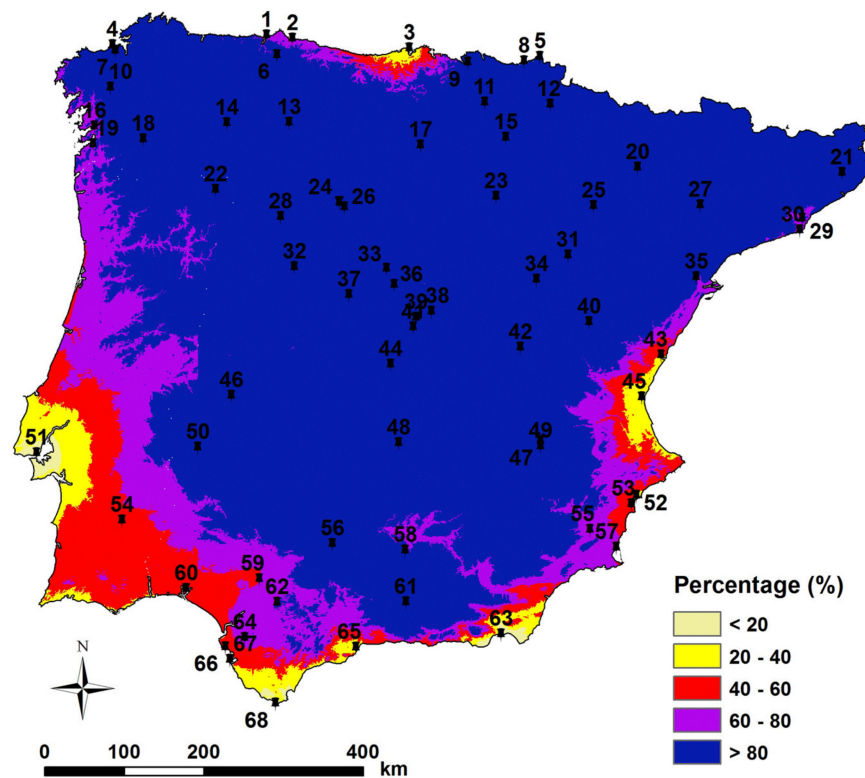


Figure 2. Spatial distribution of frost probability in the Iberian Peninsula (1975–2018).

3.2. Probabilities of Light, Moderate, and Severe Frosts

Figure 3 shows a distribution very similar to the probability of frost occurrence. The probability of severe (Figure 3c) or moderate (Figure 3b) frosts decreased on all coasts of the Peninsula, increasing the ability to grow frost-sensitive species in these areas, especially along the Mediterranean coast and in the southwest of the IP. In most of the territory, the probability of severe frosts was very high, limiting cultivation to species resistant to winter cold or periods outside the cold season. Proximity to a river (Tagus, Guadiana, Guadalquivir, and Ebro) slightly reduced the probability of severe frosts. This influence has also been described by various authors like Fridley [65] and Poteau et al. [66], who suggest that the presence of water bodies has a protective effect against the intensity and frequency of advection frosts.

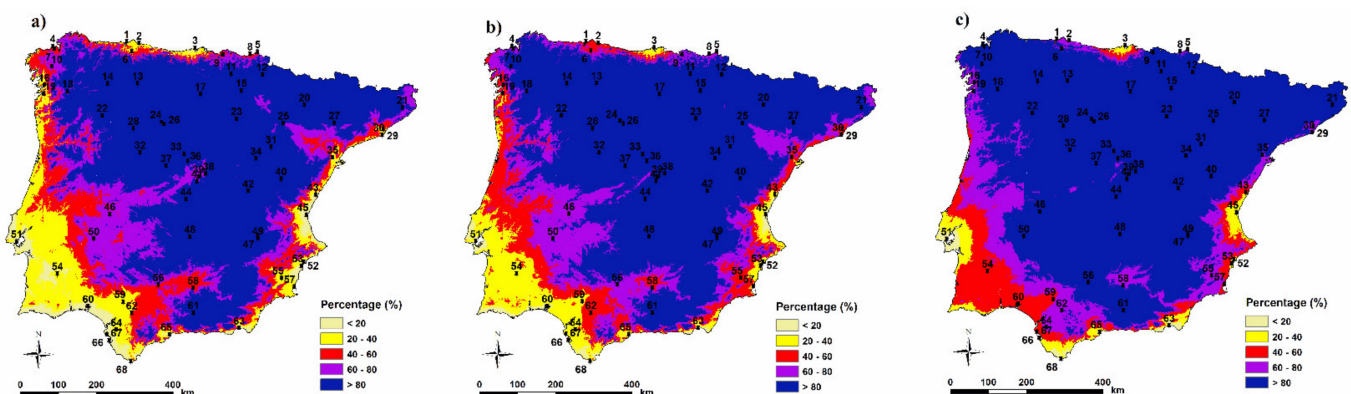


Figure 3. Spatial distribution of light (a), moderate (b), and severe (c) frosts in the Iberian Peninsula (1975–2018).

The correlations between the probabilities of different frost intensities and elevation were significant, and the correlation coefficients increased as the frost intensity increased ($r = 0.595$; $r = 0.692$; $r = 0.732$, for light, moderate, and severe frosts, respectively), emphasizing the great impact of elevation on the occurrence and intensity of frost, in line with Neuner and Hacker [67] and Neuner [68].

3.3. Mean Absolute Minimum Yearly Temperature

This index informs us of the severity of the lowest annual temperatures recorded in the selected stations, so it is of great interest for choosing crop species and varieties and their resistance to cold throughout the territory. At 55 of the 68 stations, the TN values were below zero. Molina de Aragón and Navacerrada, located on the northern plateau and at a high elevation, had the lowest values of -13.2 and -12 °C. In contrast, Tarifa, Cádiz, Almería, and Lisboa, which are all coastal stations, had the highest mean values and were above 3 °C (Table 3). TN showed a high correlation ($r = 0.855$, $p < 0.01$) with elevation.

The value of TN indicates the winter severity. We can see in Figure 4 the variability of TN across the IP. It was < -5 °C in many places and < -2.2 °C in many others, limiting perennial crops' sensitivity to winter cold.

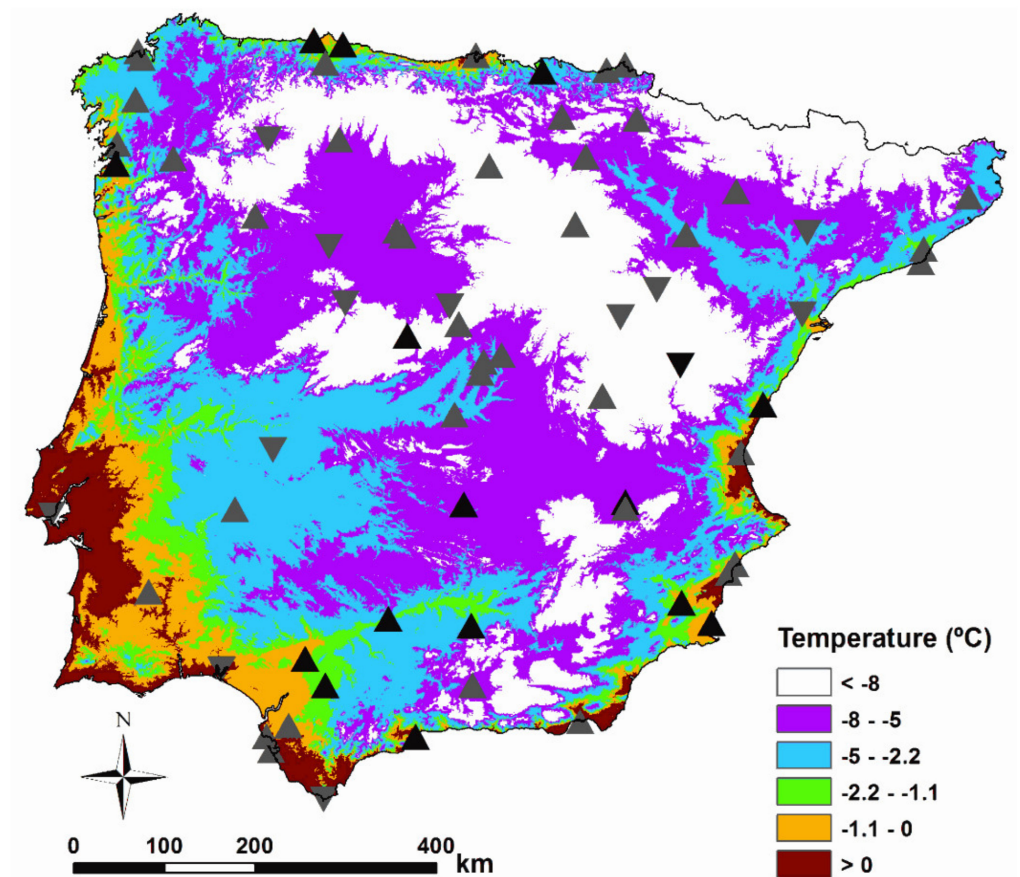


Figure 4. Spatial distribution of lowest minimum temperature (TN) in the Iberian Peninsula (1975–2018). Boldface down-pointing triangles show (negative) decreasing trends and boldface up-pointing triangles show (positive) increasing trends. Non-boldface up- and down-pointing triangles represent non-significant trends.

Table 3. Lowest minimum temperature (TN) and frost day (FD) per selected station in the Iberian Peninsula (1975–2018).

No	Station	TN				FD			N°	Station	TN			FD					
		Mean	SD	Q		Mean	SD	Q			Mean	SD	Q	Mean	SD	Q			
1	Avilés	−0.6	1.4	0.04	*	2.6	2.6	−0.07	**	35	Tortosa	−0.8	1.3	−0.00	2.9	3.0	0.00		
2	Gijón	−0.7	2.2	0.15	***	5.5	7.0	−0.24	***	36	Navacerrada	−12.0	2.4	0.01	133.0	23.2	−0.62	**	
3	Santander	1.4	1.5	0.02		0.4	1.4			37	Ávila	−9.7	2.7	0.08	*	81.0	24.9	−0.51	
4	Coruña	2.0	1.3	0.03		0.1	0.4			38	Torrejón	−6.6	1.8	0.00		50.2	17.7	−0.15	
5	Fuenterrabía	−3.6	2.1	0.04		11.4	6.4	−0.21	**	39	Madrid	−2.9	1.7	0.01		14.4	8.8	−0.11	
6	Oviedo	−2.3	1.6	0.03		8.2	5.7	−0.06		40	Teruel	−9.6	3.1	−0.13	**	86.6	20.5	0.55	
7	Alvedro	−2.4	1.3	0.02		10.4	8.2	−0.11		41	Getafe	−5.1	1.9	0.03		33.5	15.6	−0.39	
8	Igueldo	−2.6	2.0	0.01		7.0	5.0	−0.05		42	Cuenca	−7.8	2.0	0.02		61.0	18.6	−0.61	*
9	Bilbao	−2.8	1.7	0.04	*	9.1	5.9	−0.15		43	Castellón	0.3	1.7	0.07	***	1.5	2.8		
10	Santiago	−3.2	1.3	0.02		13.8	6.4	−0.13		44	Toledo	−5.3	1.7	0.01		34.5	16.6	−0.33	
11	Vitoria	−7.8	3.0	0.01		47.9	12.1	−0.03		45	Cáceres	−2.6	1.6	−0.03		10.1	6.9	0.13	
12	Pamplona	−6.6	2.5	0.03		39.2	12.9	−0.41	*	46	Valencia	1.2	1.4	0.01		0.5	1.2		
13	León	−7.8	2.3	0.00		71.5	19.5	0.03		47	Albacete	−7.1	3.1	0.07	*	45.6	18.2	−0.81	**
14	Ponferrada	−5.6	1.8	−0.03		41.5	17.5	0.08		48	Ciudad Real	−5.4	1.7	0.05	*	37.2	17.8	−0.60	**
15	Agoncillo	−5.4	1.9	0.00		26.9	11.7	0.19		49	Los Llanos	−8.2	3.1	0.00		52.6	16.6	−0.48	*
16	Pontevedra	−0.5	1.6	0.04		2.6	2.9	−0.07	*	50	Talavera la Real	−3.5	1.7	0.01		18.9	15.2	−0.17	
17	Villafria	−9.7	2.7	0.05		81.0	20.0	−0.61	**	51	Lisboa	3.1	3.4	−0.00		0.4	2.3		
18	Ourense	−4.3	1.8	0.00		26.1	13.8	−0.11		52	Alicante	0.6	1.5	0.00		0.9	1.7		
19	Vigo	−0.7	1.4	0.04	*	3.5	3.1	−0.11	**	53	Alicante	0.4	1.5	0.01		0.9	1.4	0.00	
20	Huesca	−5.9	2.1	0.01		33.2	13.4	−0.32		54	Beja	−0.5	1.7	0.02		1.9	2.3	0.00	
21	Girona	−6.1	1.9	0.00		42.0	13.7	−0.18		55	Murcia	−1.8	1.8	0.06	**	6.3	6.9	−0.26	***
22	Braganza	−6.6	2.4	0.00		48.8	16.8	−0.29		56	Córdoba	−2.9	2.2	0.06	*	13.5	12.2	−0.18	
23	Soria	−9.2	2.4	0.00		83.9	19.0	−0.31		57	San Javier	−0.9	1.6	0.06	**	3.0	3.2	−0.05	**
24	Villanubla	−8.3	1.9	0.03		78.2	20.2	−0.26		58	Jaén	−2.3	2.3	0.07	**	6.9	9.1	−0.20	**
25	Zaragoza	−4.5	1.8	0.00		21.5	10.7	−0.14		59	Sevilla	−0.5	2.0	0.10	***	3.0	5.3	−0.04	**
26	Valladolid	−6.9	2.0	0.04		57.1	19.2	−0.64	**	60	Huelva	0.4	1.6	−0.01		1.4	2.4	0.00	
27	Lleida	−6.0	2.1	−0.01		39.7	16.0	−0.01		61	Granada	−6.2	2.4	0.00		48.5	18.9	0.00	
28	Zamora	−6.0	1.8	0.00		47.4	19.3	−0.03		62	Morón la Frontera	−2.6	2.5	0.08	*	9.5	9.2	−0.27	**
29	Barcelona	−1.4	2.0	0.02		4.6	4.6	−0.07		63	Almería	3.5	2.9	0.01		0.0	0.2		
30	Barcelona	−1.2	1.8	0.01		4.3	4.7	−0.04		64	Jerez de la Frontera	−1.3	2.1	0.02		4.1	4.2	0.00	
31	Daroca	−8.8	2.4	−0.00		68.7	18.3	−0.14		65	Málaga	1.4	1.6	0.05	**	0.2	0.5		
32	Salamanca	−8.1	1.8	−0.04		75.9	21.5	0.12		66	Rota	0.2	1.8	0.00		1.4	2.2	0.00	
33	Segovia	−7.8	2.4	−0.01		53.0	17.9	−0.14		67	Cádiz	3.6	2.2	0.01		0.2	1.0		
34	Molina de Aragón	−13.2	3.3	0.00		118.3	20.1	−0.33		68	Tarifa	4.2	2.1	−0.04		0.0	0.3		

SD: Standard Deviation, Q: Sen's slope (per year). *, **, *** if trend at $p < 0.050$; 0.10; 0.01 level of significance. Empty cells denote that the Sen's test cannot be computed due to the lack of variability. Boldface indicates significant trends.

At 15 stations, significant positive trends were found throughout the historical series, with values between 0.04 °C/year in Avilés and 0.15 °C/year in Gijón. The stations with significant trends were located throughout the territory except in the western IP and were located at very different elevation ranges (4–1130 m). All this indicates a warming of winters regardless of location and elevation. In addition, the magnitude of the trend (Q) was not influenced by the elevation of the station indicating a global trend in all elevation conditions.

Abanades et al. [69] found that minimum temperatures in Spain were increasing at a rate of 0.10 °C/decade. De Lima et al. [70] found for Portugal an almost generalized trend (80% of the stations) of the temperatures of the coldest night of the year, with a magnitude of 0.5–1.0 °C/decade. Fernández-Long et al. [27] found similar results in southeaster Argentina, showing a general indication of warming in the region, mainly manifested by the increase in minimum temperatures. Similar results were found by Zeinali et al. [71] in Iran. Karl et al. [72] noted, in a study on a global scale (Northern Hemisphere), an asymmetric increase in extreme temperatures that manifested as a faster increase in minimum temperatures than in maximum temperatures. This increase in minimum temperatures is probably one of the causes of a longer FFP in Europe [73].

3.4. Frost Days

The number of frosts per year showed great variability. The average was 29 frosts for the whole IP by station per year, and the coefficient of variation between years was 90%. Navacerrada (in the center of the Peninsula and at 1894 m elevation), with 133 frosts per year, was the place where it froze the most. Tarifa and Almería (both in the south and on the coast) were the places where it froze the least, with zero frosts. The trend study revealed that practically all stations showed negative trends, indicating a reduction in frost days per year in the study period (Table 3). This trend was significant at 18 stations distributed throughout the territory, both inland and coastal, unlike that found by Fernández-Montes and Rodrigo [74]. They only reported significant trends for the stations located along the IP coast when analyzed in groups and not individually.

This tendency of the number of frosts to decrease seems to be a generalized situation globally in recent years; Easterling et al. [38] found decreasing trends in the number of frosts in Australia, China, central and northern Europe, New Zealand, and the USA. In the work of Dai et al. [75] in eastern China, 11 of 12 stations showed significant negative trends, with values of up to −5.17 days per decade. Recently, Pi et al. [76] found a reduction in the number of frosts in Northwest China of 3.71 days per decade. Piticar et al. [77] reported identical results in Chile with significant trends at most stations and reductions of up to −3.32 days per decade. The reduction rates in the number of frosts per year found in our study (Table 3) are higher than those found in the studies cited above, indicating a greater impact of global warming in the IP.

FD was highly correlated with elevation ($r = 0.911$, $p < 0.01$), and the magnitude of the trend (Q) was also correlated with elevation ($r = -0.742$, $p = 0.01$), indicating that the higher the elevation, the greater the number of frosts. The reduction in the number of frosts was more pronounced in the higher-elevation stations. This significant trend was represented by -0.6 frosts per year at stations over 400 m elevation.

The Albacete station had the most pronounced reduction (Q = −0.819 days/year, $p < 0.01$) (Table 3), due only to the reduction in severe frosts (Q = −0.523 days/year, $p < 0.001$) (Table 4), unlike in most stations, in which the reduction in the number of frosts was mainly the result of a decrease in light frosts (Table 4).

Table 4. Number of light (LF), moderate (MF), and severe frosts (SF) during the year, per selected stations in the Iberian Peninsula (1975–2018).

No	Station	LF			MF			SF			No	Station	LF			MF			SF							
		Mean	SD	Q	Mean	SD	Q	Mean	SD	Q			Mean	SD	Q	Mean	SD	Q	Mean	SD	Q					
1	Avilés	1.9	1.9	-0.06	**	0.5	0.8		0.2	0.7		35	Tortosa	1.9	1.8	0.00		0.7	1.2		0.2	0.6				
2	Gijón	3.4	3.7	-0.16	***	1.4	2.6	-0.04	***	0.7	1.7		36	Navacerrada	30.0	7.7	-0.28	**	20.5	5.2	-0.08	78.9	16.9	-0.18		
3	Santander	0.3	0.9			0.1	0.6			0.0	0.0		37	Ávila	21.8	6.7	-0.11		16.9	4.5	0.00	40.2	19.9	-0.30		
4	Coruña	0.1	0.4			0.0	0.0			0.0	0.0		38	Torrejón	13.8	4.2	-0.03		12.6	4.7	0.10	22.6	12.9	-0.27		
5	Fuenterrabía	5.8	3.6	-0.13	**	2.7	2.4	-0.05	*	2.8	2.8	0.00	39	Madrid	8.3	5.6	-0.05		3.7	2.7	-0.03	2.2	2.6	0.00		
6	Oviedo	5.2	4.3	0.00		1.6	1.5	0.00		1.1	1.6	0.00	40	Teruel	21.7	6.0	-0.24	**	17.5	4.6	-0.08	45.3	19.4	0.65	*	
7	Alvedro	6.0	4.6	-0.06		2.9	2.9	0.00		1.4	1.8	0.00	41	Getafe	13.1	4.8	-0.04		8.4	4.6	-0.10	11.2	7.7	-0.23	*	
8	Igueldo	3.6	2.7	-0.04		1.7	2.1	0.00		1.5	2.4	0.00	42	Cuenca	18.9	5.5	-0.26	***	13.1	4.0	0.00	27.8	13.2	-0.37		
9	Bilbao	4.7	2.4	-0.05		2.2	2.6	0.00		1.9	2.0	-0.03	43	Castellón	1.0	1.7			0.3	0.7		0.1	0.8			
10	Santiago de Compostela	7.8	3.7	-0.08		3.7	2.3	0.00		2.0	2.0	0.00	44	Toledo	11.2	4.9	-0.10		9.2	5.4	0.00	13.4	8.6	-0.14		
11	Vitoria	17.2	4.9	0.08		12.1	3.3	0.04		17.3	8.4	-0.14	45	Cáceres	5.1	3.5	0.04		2.7	2.7	0.00	2.0	2.5	0.02	*	
12	Pamplona	15.4	5.8	-0.23	***	9.1	4.1	-0.04		13.9	8.0	-0.10	46	Valencia	0.3	0.6			0.2	0.7		0.0	0.2			
13	León	24.4	7.5	-0.13		15.0	4.3	-0.10		29.6	13.9	0.17	47	Albacete	15.2	4.8	-0.12		9.9	4.0	-0.09	19.4	12.7	-0.52	***	
14	Ponferrada	13.2	5.1	-0.05		9.0	4.7	0.00		17.9	12.5	0.14	48	Ciudad Real	12.9	5.9	-0.14		9.1	4.6	-0.04	14.2	9.9	-0.35	**	
15	Agoncillo	11.3	4.6	0.00		6.0	3.2	0.07	*	8.6	6.4	0.10	49	Los Llanos	15.0	4.5	-0.21	***	10.7	3.2	-0.07	25.4	13.1	-0.20		
16	Pontevedra	1.8	2.1	0.00		0.6	0.8			0.2	0.9		50	Talavera la Real	7.7	5.0	-0.07		5.2	5.2	0.00	5.4	6.4	-0.04		
17	Villafria	25.1	7.4	-0.16		16.9	4.2	0.00		37.3	14.0	-0.48	*	51	Lisboa	0.0	0.0			0.0	0.0		0.4	2.3		
18	Ourense	10.6	4.6	-0.08		5.8	4.3	0.04		9.2	6.9	-0.04	52	Alicante	0.6	1.1			0.2	0.4		0.0	0.3			
19	Vigo	2.6	2.2	-0.08	**	0.6	1.1			0.2	0.9		53	Alicante	0.5	0.8			0.3	0.6		0.0	0.2			
20	Huesca	12.8	5.0	-0.16	*	7.9	4.3	-0.04		11.9	7.7	-0.09	54	Beja	1.1	1.4	0.00		0.6	1.0		0.2	0.5			
21	Girona	15.0	4.9	-0.09		11.3	4.3	-0.05		14.2	7.8	0.00	55	Murcia	3.5	3.7	-0.17	***	1.5	1.6	-0.06	***	1.2	2.4		
22	Braganza	14.8	4.9	-0.06		11.3	4.8	-0.06		21.6	11.0	-0.07	56	Córdoba	7.3	6.1	-0.13		3.1	3.0	0.00	2.8	4.5	0.00		
23	Soria	24.6	6.7	-0.20	*	16.1	5.1	-0.07		40.7	14.6	-0.12	57	San Javier	2.2	2.5	-0.04	*	0.4	0.6		0.2	0.8			
24	Villanubla	23.5	5.8	-0.09		16.1	4.4	0.00		36.4	15.8	-0.13	58	Jaén	3.8	4.7	-0.14	***	1.6	2.3	0.00	1.5	3.5	0.00		
25	Zaragoza	8.70	4.1	0.00		5.3	3.6	-0.05		7.0	5.4	-0.03	59	Sevilla	1.7	2.5	-0.03	**	0.7	1.5		0.5	1.7			
26	Valladolid	18.9	6.5	-0.23	**	13.6	5.0	-0.03		23.2	13.5	-0.37	*	60	Huelva	1.0	1.5	0.00		0.3	1.0		0.0	0.2		
27	Lleida	14.4	4.8	-0.04		9.0	4.2	0.00		15.5	9.7	0.06	61	Granada	15.4	4.9	-0.12	*	10.8	5.7	0.06	21.0	15.0	0.03		
28	Zamora	15.2	5.6	0.00		10.7	5.0	-0.05		19.4	12.8	0.13	62	Morón de la Frontera	4.9	4.1	-0.14	**	2.6	3.2	-0.05	*	1.8	3.2	0.00	+
29	Barcelona	2.40	2.3	-0.04		1.1	1.7	0.00		1.0	1.9		63	Almería	0.0	0.0			0.0	0.0		0.0	0.2			
30	Barcelona	2.60	3.0	-0.03		1.1	1.4	0.00		0.6	1.6		64	Jerez de la Frontera	2.7	2.7	0.00		0.6	1.0		0.8	1.4			
31	Daroca	18.0	4.7	-0.10		14.5	4.5	0.00		34.9	14.8	-0.12	65	Málaga	0.1	0.4			0.1	0.3		0.0	0.2			
32	Salamanca	19.6	6.7	-0.23	**	15.8	5.3	0.00		38.6	18.6	0.43	66	Rota	0.9	1.4			0.3	0.7		0.1	0.5			
33	Segovia	18.8	7.0	-0.10		12.0	4.2	0.04		21.0	10.6	0.00	67	Cádiz	0.1	0.5			0.1	0.5		0.0	0.2			
34	Molina de Aragón	22.2	5.6	-0.13		16.7	5.5	-0.09		76.4	19.5	-0.18	68	Tarifa	0.0	0.0			0.0	0.0		0.0	0.3			

SD: Standard deviation; Q: Sen's Slope (per year). *, **, *** if trend at $p < 0.050$; 0.010; 0.001 level of significance. Empty cells denote that the Sen's test cannot be computed due to the lack of variability. Bold face indicates significant trends.

The stations recorded on average more severe frosts (847.6 frosts/year) than moderate (418.2 frosts/year) and light frosts (635.5 frosts/year). The Teruel station ($Q = 0.65$ frosts/year) showed a clear positive trend. The light frosts showed significant negative trends at 19 weather stations, which were widely distributed, some with very high reductions. The significant trends were all negative, except Teruel, and were distributed throughout the study area (Figure 5).

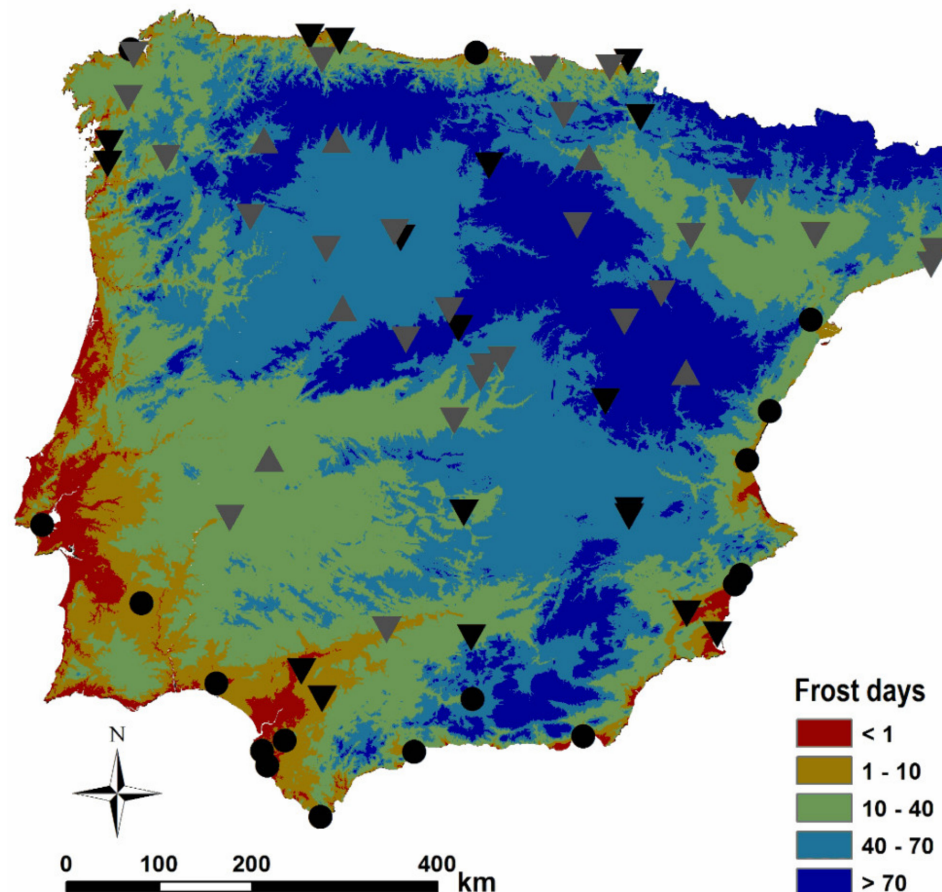


Figure 5. Spatial distribution of frost days in the Iberian Peninsula (1975–2018). Boldface down-pointing triangles show (negative) decreasing trends and boldface up-pointing triangles show (positive) increasing trends. Non-boldface up- and down-pointing triangles represent non-significant trends. Black points show the locations in which there were insufficient data to analyze trends.

3.5. Date of the First Frost

FFD showed great variability throughout the territory studied: from October 2 for Molina de Aragón (1056 m elevation) to January 23 for Alicante (3 m elevation). The Tarifa, Lisbon, and Almeria stations were omitted due to the presence of only two frosts in the study period. FFD was highly correlated with elevation ($r = -0.804$, $p < 0.01$), indicating an earlier mean FFD as the elevation increased and therefore beginning the frost period at earlier dates. The 68 stations presented significant trends (Table 5), all of them positive, indicating a tendency to delay FFD as well as the beginning of the frost period. This is an important input for deciduous perennial crops going into winter dormancy, which begin their vegetative dormancy with the first frost.

Table 5. First frost day (FFD), last frost day (LFD), and frost-free period (FFP) per selected station in the Iberian Peninsula (1975–2018).

No	Station	FFD			LFD			FFP				No	Station	FFD			LFD			FFP					
		Mean	SD	Q	Mean	SD	Q	Mean	SD	Q				Mean	SD	Q	Mean	SD	Q	Mean	SD	Q			
1	Avilés	5-ene.	27.0	0.28	28-ene.	27.1	−0.46	348	21.3	0.49	**	35	Tortosa	31-dic.	22.7	0.15	22-ene.	24.0	0.05	347	22.1				
2	Gijón	23-dic.	31.2	1.15	10-feb.	23.6	−1.00	332	38.2	1.66	***	36	Navacerrada	6-oct.	16.1	0.46	21-may.	27.6	−0.28	137	32.4	0.00	*		
3	Santander	20-ene.	28.1	0.65	23-ene.	27.8	0.44	364	1.80			37	Ávila	23-oct.	15.8	0.23	24-abr.	27.3	−0.90	**	180	34.2	0.72	**	
4	Coruña	9-ene.	4.20		11-ene.	3.5		365	0.60			38	Torrejón	12-nov.	13.4	0.32	27-mar.	22.5	−0.67	**	230	25.9	1.42	***	
5	Fuenterrabía	10-dic.	22.8	0.62	11-feb.	26.3	−0.30	303	28.3	1.08	**	39	Madrid	5-dic.	17.2	0.29	15-feb.	26.4	−0.04	295	33.0	1.08			
6	Oviedo	26-dic.	30.8	0.58	18-feb.	24.8	−0.26	315	38.7	0.72		40	Teruel	25-oct.	13.5	−0.14	16-abr.	21.6	−0.45	*	191	25.7	0.69		
7	Alvedro	17-dic.	26.2	0.49	28-feb.	30.4	−0.61	293	41.4	1.28	*	41	Getafe	24-nov.	11.2	0.23	12-mar.	27.9	−1.18	***	256	28.6	0.43	***	
8	Igueldo	26-dic.	29.5	0.11	6-feb.	27.7	−0.17	327	34.7	0.46		42	Cuenca	8-nov.	15.2	0.47	8-abr.	22.7	−0.84	***	213	30.1	1.49	***	
9	Bilbao	19-dic.	31.6	0.25	19-feb.	29.8	−0.60	304	36.4	0.81		43	Castellón	7-ene.	26.8	0.77	29-ene.	22.7	0.03	356	21.9	1.25			
10	Santiago de Compostela	28-nov.	20.2	0.33	11-mar.	29.0	−0.88	*	260	36.1	1.29	**	44	Toledo	24-nov.	14.5	0.42	13-mar.	29.1	−0.96	**	255	34.8		***
11	Viforia	5-nov.	15.5	−0.30	16-abr.	22.8	−0.83	***	202	26.4	0.67	*	45	Cáceres	14-dic.	21.3	−0.23	11-feb.	22.9	0.30	312	35.9	1.42		
12	Pamplona	15-nov.	15.4	0.16	29-mar.	24.5	−0.78	**	230	29.7	0.81	**	46	Valencia	17-ene.	24.4	0.66	19-ene.	24.5	0.61	364	1.70	−0.16		
13	León	1-nov.	13.5	−0.12	22-abr.	25.0	−0.33	192	26.3	0.30		47	Albacete	16-nov.	17.6	0.72	25-mar.	27.9	−1.30	***	234	36.7		***	
14	Ponferrada	18-nov.	13.3	0.11	21-mar.	25.5	−0.52	241	31.6	0.67		48	Ciudad Real	23-nov.	16.0	0.60	10-mar.	24.1	−1.15	***	257	32.3	2.04	***	
15	Agoncillo	17-nov.	15.0	0.33	19-mar.	22.5	−0.25	242	28.2	0.50		49	Los Llanos	10-nov.	15.2	0.55	2-abr.	24.1	−1.17	***	222	31.5	1.67	***	
16	Pontevedra	8-ene.	29.8	0.52	1-feb.	22.4	0.00	349	22.8	0.11		50	Talavera la Real	5-dic.	19.7	0.13	17-feb.	28.9	−0.94	**	293	36.3	1.76	**	
17	Villafria	19-oct.	16.4	0.21	26-abr.	24.9	−0.65	**	174	31.4	0.93	**	51	Lisboa	27-mar.	0.00		25-abr.	0.0		364	4.70	1.02		
18	Ourense	3-dic.	23.5	0.29	15-mar.	28.2	−0.46	264	38.7	1.16	*	52	Alicante	23-ene.	28.2	−0.52	3-feb.	20.1	−0.48	361	11.7				
19	Vigo	1-ene.	25.0	0.33	29-ene.	23.5	−0.51	343	26.4	0.55	*	53	Alicante	20-ene.	29.7	−0.82	3-feb.	19.7	−0.12	359	19.0				
20	Huesca	27-nov.	14.4	0.25	23-mar.	25.7	−0.75	**	248	30.8	1.32	**	54	Beja	14-ene.	23.2	0.49	31-ene.	22.1	−0.17	355	17.2	0.00		
21	Girona	20-nov.	14.9	0.33	23-mar.	23.0	−0.49	241	27.7	0.96	**	55	Murcia	24-dic.	27.6	0.88	7-feb.	27.8	−1.26	**	327	40.3	0.00	***	
22	Braganza	9-nov.	22.9	0.14	8-abr.	18.4	−0.16	215	29.3	0.37		56	Córdoba	9-dic.	23.4	0.20	10-feb.	27.7	−0.89	*	308	36.7	1.85	*	
23	Soria	27-oct.	15.6	−0.23	22-abr.	24.3	−0.68	**	187	25.9	0.48		57	San Javier	3-ene.	28.1	0.52	5-feb.	25.9	−0.63	339	35.4	1.10	**	
24	Villanubla	28-oct.	12.4	0.07	25-abr.	24.4	−0.33	*	186	25.8	0.55		58	Jaén	20-dic.	28.0	0.90	7-feb.	29.3	−0.64	325	37.3	0.10	*	
25	Zaragoza	28-nov.	15.2	0.50	*	24-feb.	24.5	−0.25	278	26.3	0.71	*	59	Sevilla	3-ene.	23.6	1.08	25-ene.	27.2	0.19	352	21.0	1.12	***	
26	Valladolid	9-nov.	18.0	0.72	**	12-abr.	26.3	−1.21	***	211	35.6	2.00	***	60	Huelva	9-ene.	21.9	−0.38	25-ene.	22.0	−0.25	358	15.7	0.08	
27	Lleida	21-nov.	14.4	0.16	11-mar.	22.1	−0.46	*	254	26.5	0.55		61	Granada	15-nov.	15.6	0.17	23-mar.	23.0	−0.60	*	236	30.2	0.00	*
28	Zamora	16-nov.	16.4	0.11	30-mar.	25.7	−0.48	*	230	31.4	0.69		62	Morón de la Frontera	15-dic.	27.7	1.06	19-feb.	31.1	−1.09	**	309	43.2	0.83	***
29	Barcelona	4-ene.	30.6	0.59	8-feb.	23.6	−0.29	337	31.6	0.25		63	Almería						365	0.20	2.53				
30	Barcelona Airport	1-ene.	35.5	0.51	6-feb.	28.3	−0.34	337	35.1	0.28		64	Jerez de la Frontera	29-dic.	26.7	0.00	30-ene.	22.9	−0.73	342	26.8				
31	Daroca	31-oct.	13.8	−0.05	13-abr.	21.4	−0.43	*	201	23.1	0.42		65	Málaga	20-ene.	28.9	1.61	26-ene.	21.5	1.12	364	6.50	0.18		
32	Salamanca	27-oct.	12.9	−0.38	15-abr.	22.6	−0.55	*	194	23.3	0.33		66	Rota	2-ene.	27.0	−0.41	20-ene.	24.7	0.47	357	18.5			
33	Segovia	10-nov.	19.8	0.27	15-abr.	26.9	−0.50	*	207	35.1	0.94	*	67	Cádiz	10-dic.	14.1		2-ene.	16.3		364	7.00	0.00		
34	Molina de Aragón	2-oct.	13.8	0.14	3-may.	23.9	0.00	151	26.3	0.25		68	Tarifa	26-ene.	0.00		28-ene.	0.0		365	0.30				

SD: Standard Deviation. Q: Sen's Slope (per year). *, **, *** if trend at $p < 0.05$; 0.01; 0.001 level of significance. Empty cells could not perform the Sen's test due to lack of variability. Boldface indicates significant trends.

Consequently, the leaf senescence could be delayed, which could increase the risk of damage by freezing at later dates when the frosts are more frequent and intense [34,78,79]. Most of the stations with significant trends were in the interior of the IP and at elevations greater than 500 m (Figure 6). The stations of Morón de la Frontera, Jaén, and Murcia presented the highest trends (1, 0.9 and 0.87 days/year), much higher (as in the previous section) than those found by other authors in Europe, Argentina, and central Chile. Moonen et al. [80] found in Piaggia (Italy) that FFD had become significantly delayed by 17 days over 122 years, from Julian day 321 (November 16) to 338 (December 3). Piticar et al. [77] found significant increasing trends for central Chile of 3–4 days/decade, very similar to those found by Moeletsi et al. [81] in South Africa and by Hosseini et al. [41] in Iran, all of which were much smaller than those found in the IP (Table 5).

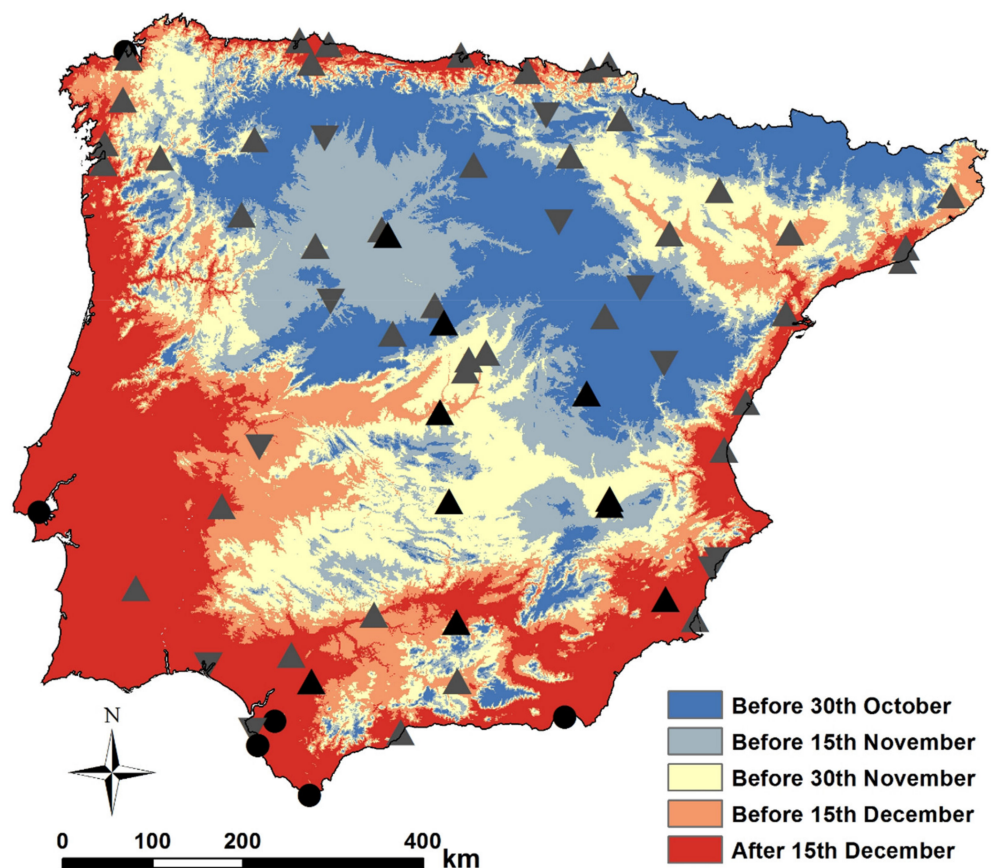


Figure 6. Spatial distribution of first frost day (FFD) in the Iberian Peninsula (1975–2018). Boldface down-pointing triangles show (negative) decreasing trends and boldface up-pointing triangles show (positive) increasing trends. Non-boldface up- and down-pointing triangles represent non-significant trends. Black points show the locations in which there were insufficient data to analyze trends.

FFD varied widely across the IP (Figure 5). The northern Meseta plateau and the mountainous systems (central and Pyrenean) received the first frost before November 15, the southern plateau around December 15, and the entire coast and southwest of the IP even later. The effect of the large rivers Tajo, Guadiana, Guadalquivir, and Ebro was also seen, as they delayed the appearance of the first frost (Figure 6). All this highlights the large differences at the beginning of the cold period, which is useful information for reducing the risk of frost damage, as indicated by Tait and Zheng [82], Rahimi et al. [83], and Varshavian et al. [84], and can have great repercussions on the phenology of crops and agricultural work.

3.6. Date of the Last Frost

LFD showed a high correlation with elevation ($r = 0.835$, $p < 0.01$), indicating delayed dates as elevation increased and therefore implying a longer frost period due to the elevation. The station with the date of the last earliest average frost was Cádiz in the Peninsular south and with the lowest elevation of all (1 m); however, the station with the latest frost was Navacerrada on May 21, located in the center of the IP, and the highest elevation station (1894 m) (Table 5). Only in 64% of the stations did the last frost occur before the onset of spring, indicating a high probability of frost damage in spring and summer crops.

LFD showed a clear significant tendency to advancement (negative) at 28 of the 69 stations (Table 5). This trend varied between -0.429 days/year for the Daroca station and -1.29 days/year for Albacete. These data are similar to those found by Hosseini et al. [41] in Iran; Moonen et al. [80] in Italy; Scheifinger et al. [85] in central Europe; Menzel et al. [73] in Germany, Austria, Switzerland, and Estonia; Varshavian et al. [84] in Iran; Fernández-Long et al. [27] in Argentina; and Piticar et al. [77] in central Chile. However, the magnitude of the trend was much greater in the IP than those places, indicating a greater impact of climate change on the frost regime. This could also be because our study incorporates the most recent years of available data, which could indicate a worsening of climate change in terms of frost in the last decade.

Contrary to what was found by Vitasse et al. [18] in Switzerland, where the highest stations (800 m) presented no significant trends, we found that seven out of ten stations located above this elevation showed significant trends of LFD advancement. As those authors indicate, if the plant phenology at these stations (over 800 m) advances at a faster pace, both phenomena will contribute to a greater risk of frost in these areas.

None of the weather stations studied showed a significant positive trend of LFD delay, which indicates a clear sign throughout the territory studied of an early start and possible lengthening of the FFP and therefore of spring cultivation. The magnitude of the trend did not show a significant correlation with elevation (data not shown), indicating that this magnitude is independent of elevation.

Figure 7 Shows that practically the entire Mediterranean coastal area, as well as much of the southwest of the IP and the depression of the Ebro River, experienced its last frost before February 28 (day 59 of the year). In contrast, in the northern and eastern plateau of the IP, as well as the mountain systems, this date extended until April 15 or beyond, a month and a half later. The stations with significant trends were distributed throughout, except in the coastal area.

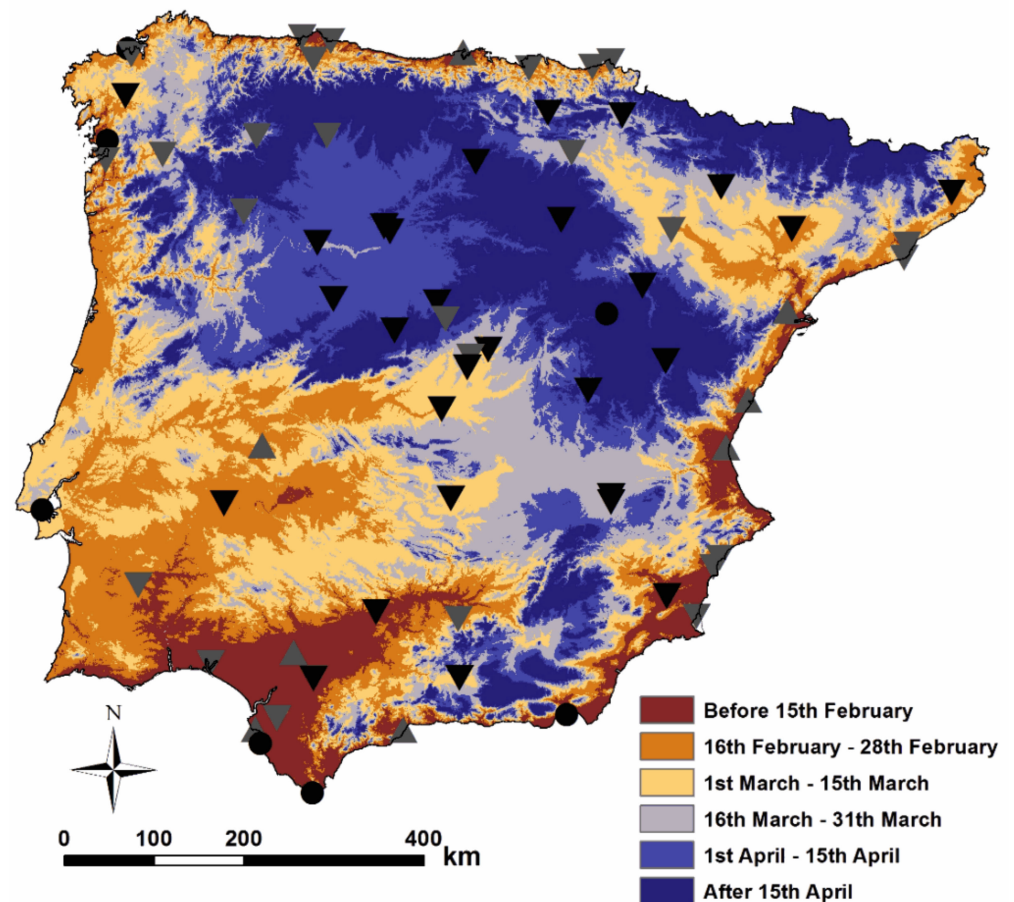


Figure 7. Spatial distribution of last frost day (LFD) in the Iberian Peninsula (1975–2018). Boldface down-pointing triangles show (negative) decreasing trends and boldface up-pointing triangles show (positive) increasing trends. Non-boldface up- and down-pointing triangles represent non-significant trends. Black points show the locations in which there were insufficient data to analyze trends.

3.7. Frost-Free Period

FFP was strongly influenced by the behavior of the previous two variables (FFD and LFD) since generalized trends of delayed FFD and advanced LFD were found, which implies a shorter frost period and therefore a longer FFP. A total of 55/68 stations showed positive trends, 32 of which were significant, and only one (Cáceres) had a (nonsignificant) negative trend (Table 5). In eight stations, there were two significant trends at the same time: A delay in the first frost and advancement of the last frost. These stations were Murcia, Morón de la Frontera, Ciudad Real, Toledo, Albacete, Los Llanos, Cuenca, and Valladolid, so they increased their FFP for both reasons, with a very strong significance ($p < 0.005$) and with a strong trend, especially the Morón de la Frontera station (2.5 days/year). The stations with significant trends were distributed across the entire geographic area and all elevations, strengthening our conclusion of a generalized trend of a longer FFP (Figure 8). The magnitude of the trend was not influenced by elevation or geographical location.

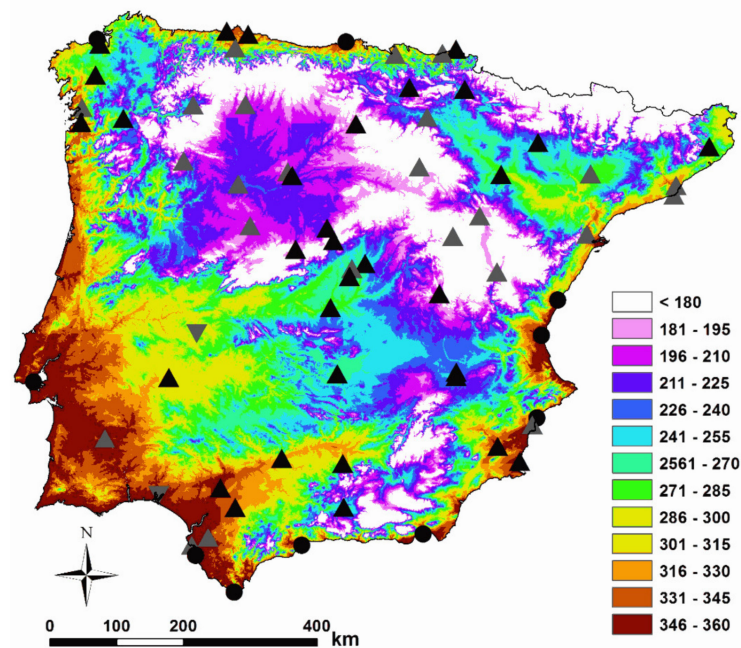


Figure 8. Spatial distribution of frost free-period (days) in the Iberian Peninsula (1975–2018). Boldface down-pointing triangles show (negative) decreasing trends and boldface up-pointing triangles show (positive) increasing trends. Non-boldface up- and down-pointing triangles represent non-significant trends. Black points show the locations in which there were insufficient data to analyze trends.

Numerous authors have found similar results across the world. For example, Moonen et al. [80] found an increase of 47 days over 122 years in Italy, due to both the delay in the first autumn frost and the advancement of the last spring frost. In the same way, Fernández-Long et al. [27] found a shortening of the frost period and therefore a lengthening of FFP of 7 days/decade in Argentina. The same was found by Potot et al. [86] in the Czech Republic (3.9 days/decade), Moeletesi et al. [81] in South Africa (1–5 days/decade), and Piticar et al. [77] in Argentina (1.20–3.33 days/decade), indicating that global warming could be the cause of all these trends by affecting minimum temperatures. However, Crimp et al. [41] found an increase in the frost period in some regions of Australia, despite the warming recorded. The lengthening of the frost-free period could increase the potential for the expansion of land use for cultivation, for example for vines [43]. Genovese et al. [87] estimated the increase in FFP for the central and southern IP at 0.5–0.7 days per year, which was the highest in Europe. In our study, 50% of the stations exceeded these values (Table 5). This increase in FFP could induce an increase in the risk of frost within the growing season, especially in Europe and especially in spring [36], due to phenological changes in crops, mainly earlier budding. This is corroborated by Menzel et al. [73], who indicated that the phenology of wild plants, as well as the dates of crop operations, advanced by 1 to 2 weeks from 1980 to the 2000s in Germany. Dai et al. [75] indicated that the date of flowering has advanced between 1.5 and 2.2 days per decade in eastern China since 1963. On the other hand, a longer period of growth (due to a shorter period of frost) could lead to an increase in productivity in the Northern Hemisphere in the context of global warming [88,89].

The relative importance of LFD advancement was greater than that of the FFD delay, since in 13 stations the longer FFP was clearly due to advancement of the last frost (Córdoba, Talavera la Real, Santiago de Compostela, Getafe, Granada, Girona, Huesca, Torrejón, Pamplona, Segovia, Vitoria, Ávila, and Villafría), while only in three stations was it clearly due to the delay of the first frost (Jaén, Zaragoza and Navarra). In the rest of the stations, the reason for this increase was not clear. FFP varied between 365 days (Almería) and 137 days (Navacerrada), showing great variability (standard deviation = 66.7 days).

FFP tended to be shorter as the elevation increased, in line with what was found by Geiger et al. [90]. This index was highly correlated with elevation ($r = -0.874$, $p < 0.001$) (Table 5). Figure 7 shows the great variability this index presents in the IP, where the mountainous areas and the central zone have less than 180 days without frost (3 months). However, the southwest of the IP and the coasts have more than 271 days (9 months) without frost, which is an important characteristic in crop productivity and land suitability for agriculture and livestock use.

4. Conclusions

The IP, despite its location in a temperate zone, has a high probability of frost occurrence in most of its territory. However, this probability is drastically lower in the southwest and along the Mediterranean coast. The reduction in the number of frosts has been more pronounced at the higher-elevation stations. The minimum temperatures recorded in the stations show a general increase throughout the territory and regardless of the elevation of the meteorological stations. This indicates a clear sign of winter warming across the IP.

The number of frosts per year was significantly reduced throughout the territory. There was a clear delay in the appearance of the first autumn frost and advancement of the last spring frost. As a result of these two situations, FFP is lengthening significantly, with values much higher than those observed in other parts of the world. Increasing FFP can also lead to improved growing conditions for heat-loving crops and the extent of the area where they can be grown.

The impact of these trends will force adaptations in the planning of the ideal planting dates, as well as a change to varieties and even species better adapted to less severe winters and the different average frost dates. Detailed information will allow farmers a better choice of varieties, appropriate cultivation dates, and optimal cultivation techniques to this changing situation.

Author Contributions: Conceptualization A.G.-M., M.A.R., and L.L.P.; methodology, A.G.-M., L.L.P., and M.A.R. software, F.J.R.; validation, F.J.M., L.L.P., and A.G.-M.; formal analysis, F.J.M., L.L.P., and F.J.R.; investigation, F.J.M., L.L.P., F.J.R., and A.G.-M.; resources, A.G.-M. and M.A.R.; data curation, L.L.P.; writing—original draft preparation, A.G.-M.; writing—review and editing, A.G.-M.; visualization, L.L.P. and F.J.R.; supervision, F.J.M.; project administration, L.L.P. and A.G.-M.; funding acquisition, F.J.M., M.A.R., and A.G.-M. All authors have read and agreed to the published version of the manuscript.

Funding: This research was funded by the Junta de Extremadura and the European Regional Development Fund (ERDF) through the projects GR18086 (Research Group TIC008), GR18088 (Research Group RNM028), and GR18011 (Research Group RNM011).

Institutional Review Board Statement: Not applicable.

Informed Consent Statement: Not applicable.

Data Availability Statement: Publicly available datasets were used to compute all climate indices used in this study. These raw data can be found here: <https://www.ecad.eu/dailydata/index.php> (accessed on 20 August 2019). Other data obtained from this source can be available from the authors as some of them are confidential.

Conflicts of Interest: The authors declare no conflict of interest. The funders had no role in the design of the study; in the collection, analyses, or interpretation of data; in the writing of the manuscript, or in the decision to publish the results.

References

1. Parker, J. Cold resistance in woody plants. *Bot. Rev.* **1963**, *29*, 123–201. [[CrossRef](#)]
2. Luo, Q. Temperature thresholds and crop production: A review. *Clim. Chang.* **2011**, *109*, 583–598. [[CrossRef](#)]
3. Hatfield, J.L.; Prueger, J.H. Temperature extremes: Effect on plant growth and development. *Weather Clim. Extrem.* **2015**, *10*, 4–10. [[CrossRef](#)]
4. Westwood, N.H. *Fruticultura de Zonas Templadas*; Mundi-Prensa: Madrid, Spain, 1982.

5. Rodrigo, J. Spring frosts in deciduous fruit trees—Morphological damage and flower hardiness. *Sci. Hortic.* **2000**, *85*, 155–173. [[CrossRef](#)]
6. Larcher, W. Effects of low temperature stress and frost injury on plant productivity. In *Physiological Processes Limiting Plant Productivity*; Johnson, C.B., Ed.; Butterworth: London, UK, 1981; pp. 253–269.
7. Larcher, W.; Bauer, H. Ecological significance of resistance to low temperature. In *Physiological Plant Ecology I: Responses to the Physical Environment*; Lange, O.L., Nobel, P.S., Osmond, C.B., Ziegler, H., Eds.; Springer: Berlin/Heidelberg, Germany, 1981; pp. 403–437.
8. Woodward, F.I.; Williams, B.G. Climate and plant distribution at global and local scales. *Vegetatio* **1987**, *69*, 189–197. [[CrossRef](#)]
9. Lyons, J.M. Chilling injury in plants. *Annu. Rev. Plant Physiol.* **1973**, *24*, 445–466. [[CrossRef](#)]
10. Pearce, R. Plant freezing and damage. *Ann. Bot.* **2001**, *87*, 417–424. [[CrossRef](#)]
11. Snyder, R.L.; Melo-Abreu, J.D. Frost protection: Fundamentals, practice and economics. *Frost Prot. Fundam. Pract. Econ.* **2005**, *1*, 1–240.
12. Rieger, M. Freeze protection for horticultural crops. *Hort. Rev.* **1989**, *11*, 45–109. [[CrossRef](#)]
13. Augspurger, C.K. Spring 2007 warmth and frost: Phenology, damage and refoliation in a temperate deciduous forest. *Funct. Ecol.* **2009**, *23*, 1031–1039. [[CrossRef](#)]
14. Gu, L.; Hanson, P.J.; Post, W.M.; Kaiser, D.P.; Yang, B.; Nemani, R.; Pallardy, S.G.; Meyers, T. The 2007 Eastern US spring freeze: Increased cold damage in a warming world? *BioScience* **2008**, *58*, 253–262. [[CrossRef](#)]
15. Hufkens, K.; Friedl, M.A.; Keenan, T.F.; Sonnentag, O.; Bailey, A.; O’Keefe, J.; Richardson, A.D. Ecological impacts of a widespread frost event following early spring leaf-out. *Glob. Chang. Biol.* **2012**, *18*, 2365–2377. [[CrossRef](#)]
16. Ningre, F.; Colin, F. Frost damage on the terminal shoot as a risk factor of fork incidence on common beech (*Fagus sylvatica* L.). *Ann. For. Sci.* **2007**, *64*, 79–86. [[CrossRef](#)]
17. Kreyling, J.; Thiel, D.; Nagy, L.; Jentsch, A.; Huber, G.; Konnert, M.; Beierkuhnlein, C. Late frost sensitivity of juvenile *Fagus sylvatica* L. differs between Southern Germany and Bulgaria and depends on preceding air temperature. *Eur. J. For. Res.* **2012**, *131*, 717–725. [[CrossRef](#)]
18. Vitasse, Y.; Schneider, L.; Rixen, C.; Christen, D.; Rebetez, M. Increase in the risk of exposure of forest and fruit trees to spring frosts at higher elevations in Switzerland over the last four decades. *Agric. For. Meteorol.* **2018**, *248*, 60–69. [[CrossRef](#)]
19. Agrosegueros 2018. Agrupación Española de Entidades Aseguradoras de los Seguros Agrarios Combinados S.A. Informe de Siniestralidades. 2018. Available online: https://agroseguero.es/fileadmin/propietario/Home/INFORMES_SINIESTRALIDAD/0_Informe_TOTAL_SINIESTRALIDADES_2018_30_septiembre_2018.pdf (accessed on 30 August 2019).
20. Agrosegueros 2019. Agrupación Española de Entidades Aseguradoras de los Seguros Agrarios Combinados S.A. Informe de Siniestralidades. 2019. Available online: https://agroseguero.es/fileadmin/propietario/Home/INFORMES_SINIESTRALIDAD/WEB_Informe_TOTAL_SINIESTRALIDADES_2019_31_agosto_2019.pdf (accessed on 30 August 2019).
21. Raper, C.D.; Kramer, P.J. Soybeans: Improvement, production and uses. *Stress Physiol. Agron. Monogr.* **1987**, *16*, 589–641.
22. Otegui, M.E.; Pereira, M.L. Fecha de siembra. In *Producción de Granos*; Bases funcionales para su manejo; Satorre, E.H., Arnold, R.L., Slafer, G.A., Fuente, E.B., Miralles, D.J., Otegui, M.E., Savin, R., Eds.; UBA: Buenos Aires, Argentina, 2003; pp. 259–275.
23. Giannakopoulos, C.; Le Sager, P.; Bindi, M.; Moriondo, M.; Kostopoulou, E.; Goodess, C.M. Climatic changes and associated impacts in the mediterranean resulting from a 2 °C global warming. *Glob. Planet. Chang.* **2009**, *68*, 209–224. [[CrossRef](#)]
24. Lionello, P.; Abrantes, F.; Gacic, M.; Planton, S.; Trigo, R.; Ulbrich, U. The climate of the Mediterranean region: Research progress and climate change impacts. *Reg. Environ. Chang.* **2014**, *14*, 1679–1684. [[CrossRef](#)]
25. Kim, G.U.; Seo, K.H.; Chen, D. Climate change over the Mediterranean and current destruction of marine ecosystem. *Sci. Rep.* **2019**, *9*, 1–9. [[CrossRef](#)] [[PubMed](#)]
26. Robeson, S.M. Increasing growing-season length in Illinois during the 20th century. *Clim. Chang.* **2002**, *52*, 219–238. [[CrossRef](#)]
27. Fernández-Long, M.E.; Müller, G.V.; Beltrán-Przekurat, A.; Scarpati, O.E. Long-term and recent changes in temperature-based agroclimatic indices in Argentina. *Int. J. Clim.* **2013**, *33*, 1673–1686. [[CrossRef](#)]
28. Yu, Q.; Li, L.; Luo, Q.; Eamus, D.; Xu, S.; Chen, C.; Wang, E.; Liu, J.; Nielsen, D.C. Year patterns of climate impact on wheat yields. *Int. J. Clim.* **2014**, *34*, 518–528. [[CrossRef](#)]
29. Menzel, A.; Fabian, P. Growing season extended in Europe. *Nature* **1999**, *397*, 659. [[CrossRef](#)]
30. Parmesan, C.; Yohe, G. A globally coherent fingerprint of climate change impacts across natural systems. *Nature* **2003**, *421*, 37–42. [[CrossRef](#)]
31. Badeck, F.W.; Bondeau, A.; Böttcher, K.; Doktor, D.; Lucht, W.; Schaber, J.; Sitch, S. Responses of spring phenology to climate change. *New Phytol.* **2004**, *162*, 295–309. [[CrossRef](#)]
32. Ge, Q.; Dai, J.; Cui, H.; Wang, H. Spatiotemporal variability in start and end of growing season in China related to climate variability. *Remote Sens.* **2016**, *8*, 433. [[CrossRef](#)]
33. Cleland, E.; Chuine, I.; Menzel, A.; Mooney, H.; Schwartz, M. Shifting plant phenology in response to global change. *Trends Ecol. Evol.* **2007**, *22*, 357–365. [[CrossRef](#)]
34. Menzel, A.; Sparks, T.H.; Estrella, N.; Koch, E.; Aasa, A.; Ahas, R.; Alm-Kübler, K.; Bissolli, P.; Braslavská, O.; Briede, A.; et al. European phenological response to climate change matches the warming pattern. *Glob. Chang. Biol.* **2006**, *12*, 1969–1976. [[CrossRef](#)]

35. Han, H.; Bai, J.; Ma, G.; Yan, J. Vegetation phenological changes in multiple landforms and responses to climate change. *ISPRS Int. J. Geo-Inf.* **2020**, *9*, 111. [[CrossRef](#)]
36. Liu, Q.; Piao, S.; Janssens, I.A.; Fu, Y.; Peng, S.; Lian, X.; Ciais, P.; Myneni, R.B.; Peñuelas, J.; Wang, T. Extension of the growing season increases vegetation exposure to frost. *Nat. Commun.* **2018**, *9*, 426. [[CrossRef](#)]
37. Matiu, M.; Ankerst, D.P.; Menzel, A. Asymmetric trends in seasonal temperature variability in instrumental records from ten stations in Switzerland, Germany and the UK from 1864 to 2012. *Int. J. Clim.* **2016**, *36*, 13–27. [[CrossRef](#)]
38. Easterling, D.R.; Evans, J.L.; Groisman, P.Y.; Karl, T.R.; Kunkel, K.E.; Ambenje, P. Observed variability and trends in extreme climate events: A brief review. *Bull. Am. Meteorol. Soc.* **2000**, *81*, 417–425. [[CrossRef](#)]
39. Bootsma, A. Estimating minimum temperature and climatological freeze risk in hilly terrain. *Agric. Meteorol.* **1976**, *16*, 425–443. [[CrossRef](#)]
40. Laughlin, G.P.; Kalma, J.D. Frost hazard assessment from local weather and terrain data. *Agric. For. Meteorol.* **1987**, *40*, 1–16. [[CrossRef](#)]
41. Crimp, S.J.; Gobbett, D.; Kokic, P.; Nidumolu, U.; Howden, M.; Nicholls, N. Recent seasonal and long-term changes in southern Australian frost occurrence. *Clim. Chang.* **2016**, *139*, 115–128. [[CrossRef](#)]
42. Hosseini, S.M.; Karbalaee, A.; Hosseini, S.A. Spatiotemporal changes of early fall and late spring frost and its trend based on daily minimum temperature in Iran. *Arab. J. Geosci.* **2021**, *14*, 304. [[CrossRef](#)]
43. Gobbett, D.; Nidumolu, U.; Crimp, S. Modelling frost generates insights for managing risk of minimum temperature extremes. *Weather Clim. Extrem.* **2020**, *27*, 100176. [[CrossRef](#)]
44. Gobbett, D.; Nidumolu, U.; Jin, H.; Hayman, P.; Gallant, J. Minimum temperature mapping augments Australian grain farmers' knowledge of frost. *Agric. For. Meteorol.* **2021**, *304*, 108422. [[CrossRef](#)]
45. Srivastava, P.K.; Pandey, P.C.; Kumar, P.; Raghubanshi, A.S.; Han, D. *Geospatial Technology for Water Resource Applications*; CRC Press: Boca Raton, FL, USA, 2016.
46. Beck, H.; Zimmermann, N.; McVicar, T.; Vergopolan, N.; Berg, A.; Wood, E.F. Present and future Köppen-Geiger climate classification maps at 1-km resolution. *Sci. Data* **2018**, *5*, 180214. [[CrossRef](#)]
47. AEMET. *Iberian Climate Atlas: Air Temperature and Precipitation (1971e2000)*; Ministerio de Medio Ambiente, Medio Rural y Marino: Madrid, Spain, 2011.
48. *ECA&D Algorithm Basis Document (ATBD)*; Royal Netherlands Meteorological Institute KNMI: De Bilt, The Netherlands, 2013.
49. Klein-Tank, A.M.; Wijngaard, J.B.; Können, G.P.; Böhm, R.; Demarée, G.; Gocheva, A.; Mileta, M.; Pashiardis, S.; Hejkrlik, L.; Kern-Hansen, C.; et al. Daily dataset of 20th-century surface air temperature and precipitation series for the European climate assessment. *Int. J. Clim.* **2002**, *22*, 1441–1453. [[CrossRef](#)]
50. Haylock, M.R.; Hofstra, N.; Klein-Tank, A.M.; Klok, E.J.; Jones, P.D.; New, M. A European daily high-resolution gridded data set of surface temperature and precipitation for 1950–2006. *J. Geophys. Res. Atmos.* **2008**, *113*. [[CrossRef](#)]
51. Wijngaard, J.B.; Klein Tank, A.M.; Können, G.P. Homogeneity of 20th century European daily temperature and precipitation series. *Int. J. Clim.* **2003**, *23*, 679–692. [[CrossRef](#)]
52. *WMO Guide to Climatological Practices, No. 100*; World Meteorological Organization: Geneva, Switzerland, 2011.
53. Allen, R.G.; Pereira, L.S.; Raes, D.; Smith, M. Crop evapotranspiration. In *Guidelines for Computing Crop Water Requirements*; FAO irrigation and drainage paper, No. 56; FAO: Rome, Italy, 1998.
54. Goovaerts, P. Using elevation to aid the geostatistical mapping of rainfall erosivity. *Catena* **1999**, *34*, 227–242. [[CrossRef](#)]
55. Hornstein, R.A. *Freezing Temperature Probabilities at Experimental Farms in the Maritime Provinces*; Meteorol. Branch Circ. 3411, Tec. 337; Canada Department Transport: Toronto, ON, Canada, 1960.
56. Ouellet, C.E. Préparation et usage des tables de probabilité de gelée. *Agriculture* **1962**, *19*, 105–111.
57. WMO. *Protection against Frost Damage*; No. 100, TP. 60; WMO, World Meteorological Organization: Geneva, Switzerland, 1963.
58. Mann, H.B. Nonparametric tests against trend. *Econometrica* **1945**, *13*, 245–259. [[CrossRef](#)]
59. Kendall, M.G. *Rank Correlation Methods*; Charles Griffin: London, UK, 1975.
60. WMO. Volume II—Management of water resources and application of hydrological practices. In *Guide to Hydrological Practices*; WMO-No. 168; World Meteorological Organization: Geneva, Switzerland, 2009.
61. Sen, P.K. Estimates of the regression coefficient based on Kendall's Tau. *J. Am. Stat. Assoc.* **1968**, *63*, 1379–1389. [[CrossRef](#)]
62. Salmi, T.; Määtä, A.; Anttila, P.; Ruoho-Airola, T.; Amnell, T. *Detecting Trends of Annual Values of Atmospheric Pollutants by the Mann-Kendall Test and Sen's Slope Estimates—the Excel Template Application MAKESENS*; Publication on Air Quality, Finnish Meteorological Institute: Helsinki, Finland, 2002.
63. Moeletsi, M.; Tongwane, M. Spatiotemporal Variation of Frost within Growing Periods. *Adv. Meteorol.* **2017**, *2017*, 5472869. [[CrossRef](#)]
64. Núñez, L.M.; Moreno, J.V.; Chazarra, A.; Abaroa, T.G.; Avello, E.; Botey, M.R. *Mapas de Riesgo: Heladas y Horas de Frío en la España Peninsular (Periodo 2002–2012)*; Ministerio de Agricultura, Alimentación y Medio Ambiente, Ed.; Agencia Estatal de Meteorología: Madrid, Spain, 2015.
65. Fridley, J.D. Downscaling climate over complex terrain: High finescale (<1000 m) spatial variation of near-ground temperatures in a montane forested landscape (Great Smoky Mountains). *J. Appl. Meteorol. Climatol.* **2009**, *48*, 1033–1049. [[CrossRef](#)]

66. Pouteau, R.; Rambal, S.; Ratte, J.P.; Gogé, F.; Joffre, R.; Winkel, T. Downscaling MODIS-derived maps using GIS and boosted regression trees: The case of frost occurrence over the arid Andean highlands of Bolivia. *Remote Sens. Environ.* **2011**, *115*, 117–129. [[CrossRef](#)]
67. Neuner, G.; Hacker, J. Ice Formation and propagation in alpine plants. In *Plants in Alpine Regions: Cell Physiology of Adaption and Survival Strategies*; Lütz, C., Ed.; Springer: Vienna, Austria, 2012; pp. 163–174.
68. Neuner, G. Frost resistance in alpine woody plants. *Front. Plant Sci.* **2014**, *5*, 654. [[CrossRef](#)]
69. Abanades, J.C.; Prats, J.C.; de Lucas, M.C.; García, F.F.; Zulaica, C.G.; De Marcos, L.G. *El Cambio Climático en España. Estado de Situación*; Documento Resumen; Instituto para la Diversificación y el Ahorro de Energía (IDEA), Oficina Española de Cambio Climático (OECC): Madrid, Spain, 2007.
70. De Lima, M.I.; Santo, F.E.; Ramos, A.M.; de Lima, J.L. Recent changes in daily precipitation and surface air temperature extremes in mainland Portugal, in the period 1941–2007. *Atmos. Res.* **2013**, *127*, 195–209. [[CrossRef](#)]
71. Zeinali, B.; Teymouri, M.; Asghari, S.; Mohammadi, M.; Gupta, V. A study of frost occurrence and minimum temperatures in Iran. *J. Earth Syst. Sci.* **2019**, *128*, 134. [[CrossRef](#)]
72. Karl, T.R.; Knight, R.W.; Gallo, K.P.; Peterson, T.C.; Jones, P.D.; Kukla, G.; Plummer, N.; Razuvayev, V.; Lindsey, J.; Charlson, R.J. A new perspective on recent global warming: Asymmetric trends of daily maximum and minimum temperature. *Bull. Am. Meteorol. Soc.* **1993**, *74*, 1007–1023. [[CrossRef](#)]
73. Menzel, A.; Jakobi, G.; Ahas, R.; Scheifinger, H.; Estrella, N. Variations of the climatological growing season (1951–2000) in Germany compared with other countries. *Int. J. Clim.* **2003**, *23*, 793–812. [[CrossRef](#)]
74. Fernández-Montes, S.; Rodrigo, F.S. Trends in seasonal indices of daily temperature extremes in the Iberian Peninsula, 1929–2005. *Int. J. Clim.* **2012**, *32*, 2320–2332. [[CrossRef](#)]
75. Dai, J.; Wang, H.; Ge, Q. The decreasing spring frost risks during the flowering period for woody plants in temperate area of eastern China over past 50 years. *J. Geogr. Sci.* **2013**, *23*, 641–652. [[CrossRef](#)]
76. Pi, Y.; Yu, Y.; Zhang, Y.; Xu, C.; Yu, R. Extreme Temperature Events during 1960–2017 in the Arid Region of Northwest China: Spatiotemporal Dynamics and Associated Large-Scale Atmospheric Circulation. *Sustainability* **2020**, *12*, 1198. [[CrossRef](#)]
77. Piticar, A. Changes in agro-climatic indices related to temperature in Central Chile. *Int. J. Biometeorol.* **2019**, *63*, 499–510. [[CrossRef](#)] [[PubMed](#)]
78. Christensen, J.H.; Christensen, O.B. A summary of the PRUDENCE model projections of changes in European climate by the end of this century. *Clim. Chang.* **2007**, *81*, 7–30. [[CrossRef](#)]
79. *IPCC 2013 Climate Change; The Physical Science Basis*; IPCC: Geneva, Switzerland, 2013.
80. Moonen, A.C.; Ercoli, L.; Mariotti, M.; Masoni, A. Climate change in Italy indicated by agrometeorological indices over 122 years. *Agric. For. Meteorol.* **2002**, *111*, 13–27. [[CrossRef](#)]
81. Moeletsi, M.E.; Tongwane, M.; Tsubo, M. The study of frost occurrence in Free State Province of South Africa. *Adv. Meteorol.* **2016**, *2016*, 9586150. [[CrossRef](#)]
82. Tait, A.; Zheng, X. Mapping frost occurrence using satellite data. *J. Appl. Meteorol.* **2003**, *42*, 193–203. [[CrossRef](#)]
83. Rahimi, M.; Hajjam, S.; Khalili, A.; Kamali, G.A.; Stigter, C.J. Risk analysis of first and last frost occurrences in the Central Alborz region, Iran. *Int. J. Clim.* **2007**, *27*, 349–356. [[CrossRef](#)]
84. Varshavian, V.; Ghahreman, N.; Khalili, A.; Hajjam, S. Statistical analysis of first and last frost occurrences and length of frost free period during the past decades in different regions of Iran. *Environ. Inform. Arch.* **2007**, *5*, 631–637.
85. Scheifinger, H.; Menzel, A.; Koch, E.; Peter, C. Trends of spring time frost events and phenological dates in Central Europe. *Theor. Appl. Clim.* **2003**, *74*, 41–51. [[CrossRef](#)]
86. Potop, V.; Zahraniček, P.; Türkott, L.; Štěpánek, P.; Soukup, J. Risk occurrences of damaging frosts during the growing season of vegetables in the Elbe river lowland, the Czech Republic. *Nat. Hazards* **2013**, *71*, 1–19. [[CrossRef](#)]
87. Genovese, G.; Bettio, M.; Orlandi, S.; Boogaard, H.L.; Petrakos, M.; Stavropoulos, P.; Glossioti, M. Methodology of the MARS crop yield forecasting system. *Stat. Data Collect. Process. Anal.* **2004**, *4*, 21291.
88. Piao, S.; Friedlingstein, P.; Ciais, P.; Viovy, N.; Demarty, J. Growing season extension and its impact on terrestrial carbon cycle in the Northern Hemisphere over the past 2 decades. *Glob. Biogeochem. Cycles* **2007**, *21*, GB3018. [[CrossRef](#)]
89. Keenan, T.F.; Gray, J.; Friedl, M.A.; Toomey, M.; Bohrer, G.; Hollinger, D.Y.; Munger, J.W.; O’Keefe, J.; Schmid, H.P.; Wing, I.S.; et al. Net carbon uptake has increased through warming-induced changes in temperate forest phenology. *Nat. Clim. Chang.* **2014**, *4*, 598–604. [[CrossRef](#)]
90. Geiger, R.; Aron, R.H.; Todhunter, P. The microclimate of caves. In *The Climate near the Ground*; Rowman and Littlefield Publishers Inc.: Lanham, MD, USA, 2003; pp. 418–424.